COMBINED TOTAL STORM TIDE FREQUENCY ANALYSIS FOR PALM BEACH COUNTY, FLORIDA

By

R. G. Dean
T. Y. Chiu
S. Y. Wang

Sponsored By

Division of Beaches and Shores
Department of Natural Resources

Submitted By

Beaches and Shores Resource Center
Institute of Science and Public Affairs
Florida State University
Tallahassee, Florida 32306

April 1992

Table of Contents

List of Figures

List of Tables

I. INTRODUCTION

1.1 Background

In accordance with the objectives and rationale of the Florida Coastal Construction Control Line, the establishment of the line is based on the damage potential of low frequency (100 year) hurricanes. This necessitates the determination of combined total tides including storm surges, astronomical tide and dynamic wave set-up which occurs primarily inside the wave breaking zone. The objective of the present study, which is carried out for Palm Beach County, Florida, is to develop, through numerical modeling, valid estimates of the combined total storm tides for return periods of 5, 10, 20, 50, 100, 200 and 500 years.

1.2 Location and General Description of the Study Area

Figure 1 shows the location of Palm Beach County which is on the southeastern Atlantic coast of Florida. The study area consists of a 45 mile coastal area from the north county line to the south county line. The northern reaches of the county are separated from the mainland by the Intracoastal Waterway along the first 9 miles south of the Martin County line, and by the north end of Lake Worth along the next 4.8 miles. The resulting coastal barrier strip varies in width from about 300 to 7,500 ft. and in height up to about 50 ft. Lake Worth is a salt-water sound extending in a north-south direction generally parallel to the ocean shore. Its width varies from 1/4 to 1-1/2 miles, and its natural depths are generally less than 8 ft. It is connected with the ocean by two artificial cuts: Lake Worth Inlet, located about 5 miles from its northern end, and South Lake Worth Inlet, near its southern end. Palm Beach, Florida, is located on the coastal barrier island formed by the two Lake Worth Inlets. The length of the island along the shoreline between Lake Worth and South Lake Worth Inlets is about 15.6 miles. The barrier is composed principally of sand, part of which is artificial fill over former marsh areas. There are occasional outcroppings of coquina on the barrier and in the offshore area. The barrier varies in width from 250 ft. to about, 3,600 ft. and in height up to about 25 ft. The town of Palm Beach occupies about the northerly 10.5 miles of the island. The southerly 5 miles of the island are occupied by parts of the City of Lake Worth, the towns of Lantana and Manalapan and all of the towns of South Palm Beach, West Palm Beach, a resort and business center, is located on the west shore of Lake Worth opposite Palm Beach. The southern reaches of the county are separated from the mainland by the south end of Lake Worth along the northerly 0.8 mile, and by the Intra-coastal Waterway along the remaining 14.7 miles. That barrier strip varies in width from about 200 to 2,000 ft. and in height up to about 30 ft. The beaches of Palm Beach County are composed of fine sand and shell fragments, and in some location, exposed rock. The locality is shown on NOAA's Nautical Charts Nos. 11460, 11462, 11466, 11474 and Figure 1 of this report.

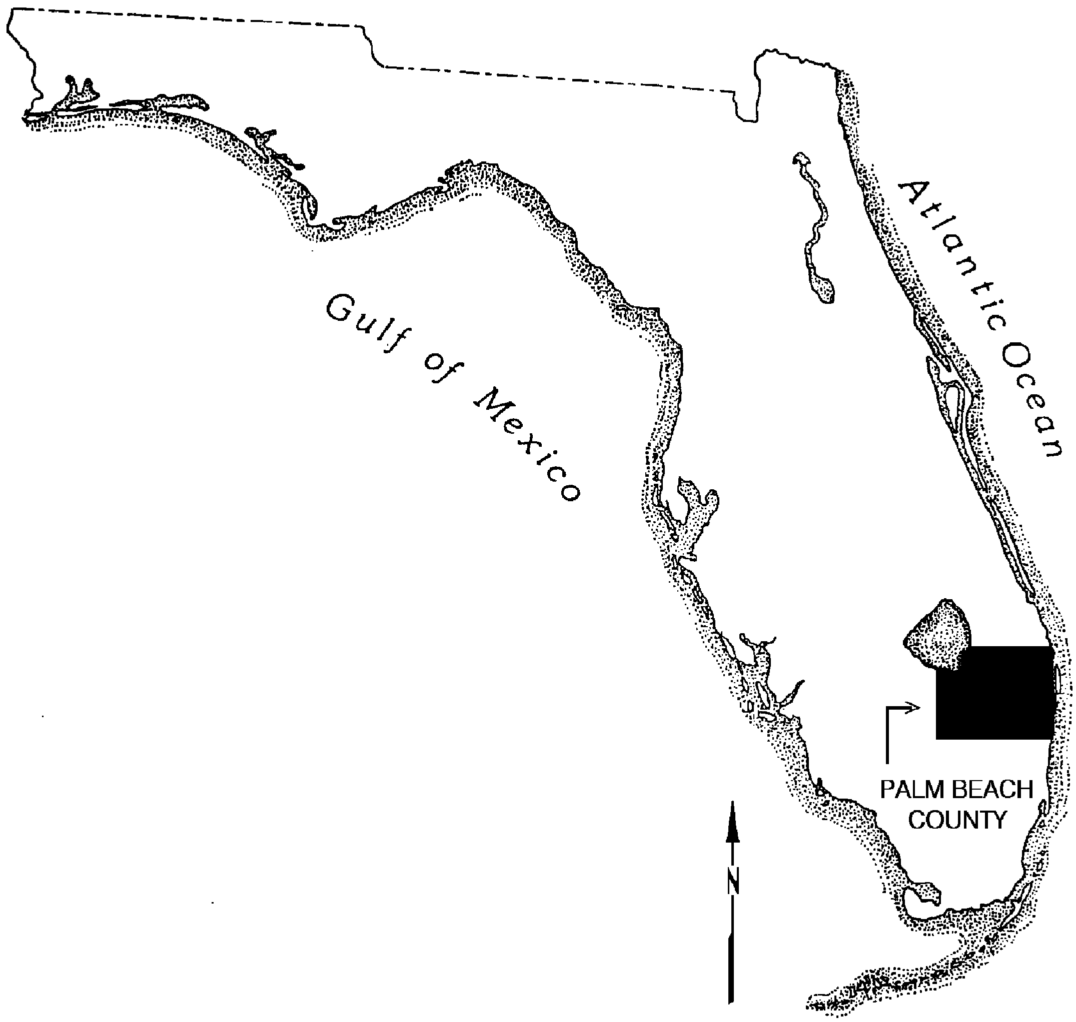

Figure 1 General Location of the Study Area

Dune elevations vary in height from less than 7 feet to over 30 feet, MSL, with gaps in the dune ridge in several places. Hurricanes and northeast storms have especially caused severe damage. A more detailed description of the study can be obtained from References (1), (2), (3) and (4)*.

1.3 Scope of the Study

The objective of the study is to develop, verify and apply a procedure which will yield valid estimates of the combined total storm tides for various return periods in the vicinity of the Palm Beach County shoreline. Throughout this report, "combined total storm tide" denotes the storm surge due to astronomical tide, wind stress and barometric pressure effects combined with the dynamic wave set-up, the latter occurring dominantly within the wave breaking zone. Available historical hurricane statistics are combined with a set of numerical

*Numbers in parentheses indicate the references listed at the end of this report.

models to simulate the storm tides at the site of interest. Tidal recordings during the hurricanes of 1926, 1945, 1947 and September 1979 (David) are employed for model calibration. Friction characteristics for various types of vegetation, buildings and underwater areas are developed to represent the actual variation of friction in the model. A simple one-dimensional model is calibrated and used to reduce the cost of computations for a large number of runs simulating a 2,000 year duration of storm tides. The dynamic wave set-up is based on analytical studies and wave tank tests.

II. HISTORICAL PROBABILITIES OF HURRICANE CHARACTERISTICS IN THE AREA OF INTEREST

2.1 Introduction and Data Source

For purposes of calculating the storm tides that occur during a long period, it is necessary to use realistic statistical representations of the important hurricane parameters: p_o (= central pressure), R (= radius to maximum winds), V_F (= forward speed), θ (= hurricane translation direction) and landfall or alongshore characteristics. The statistical parameters are based on historical hurricane data as presented in References (5) and (6). In brief, the empirical cumulative probability distributions are plotted for each of the parameters of interest and are then approximated by a series of straight line segments for computer application. All of the parameters are initially considered to be independent. The following subsections describe the statistical characteristics of the individual parameters of interest.

2.2 Hurricane Frequency and Direction

The hurricanes causing appreciable storm tides in the vicinity of the Palm Beach County shoreline are classified as "landfalling", "alongshore" or "exiting" hurricanes. Reasonably good data are available describing the characteristics of these hurricanes, from 1900 to 1987. For purposes of this report, the data contained in References (5) and (6) are merged for a 300 n.mi. segment of the coast comprising the Palm Beach County coastline. The hurricane direction is defined here as the azimuth from which the hurricane is translating at the time of landfall, or, if an alongshore hurricane, when in close proximity to the site.

The designation of a hurricane as "landfalling", "alongshore" or "exiting" is somewhat arbitrary as hurricanes travel over a continuous range of directions and there is not a particular direction relative to the shoreline for which the storm tide generating characteristics change markedly. Moreover, the one directional distribution (Figure 2) is applied for all three types of hurricanes. It is important to note that the manner in which the track of a hurricane is characterized for the purposes of this study is different for landfalling, alongshore and exiting hurricanes. For landfalling and exiting hurricanes, the track is specified by a location of landfall (or exit) and track direction, whereas for the alongshore hurricanes, the track is specified by an offshore distance and a track direction (see Section 2.5). Figure 3 presents a definition sketch of the three types of hurricanes.

For purposes of this study, landfalling and exiting hurricanes are considered to be of possible significance if they made landfall within a 300 n.mi. segment of the coast comprising the study area. This segment is extended 150 n.mi. north and south from the midpoint of the Palm Beach County shoreline. Accordingly, there are 18 landfalling and 8 exiting hurricanes. Figure 4 shows the sectors of propagation paths for the three types of hurricanes designated for Palm Beach County and the table in Appendix A lists all the hurricanes used in this study.

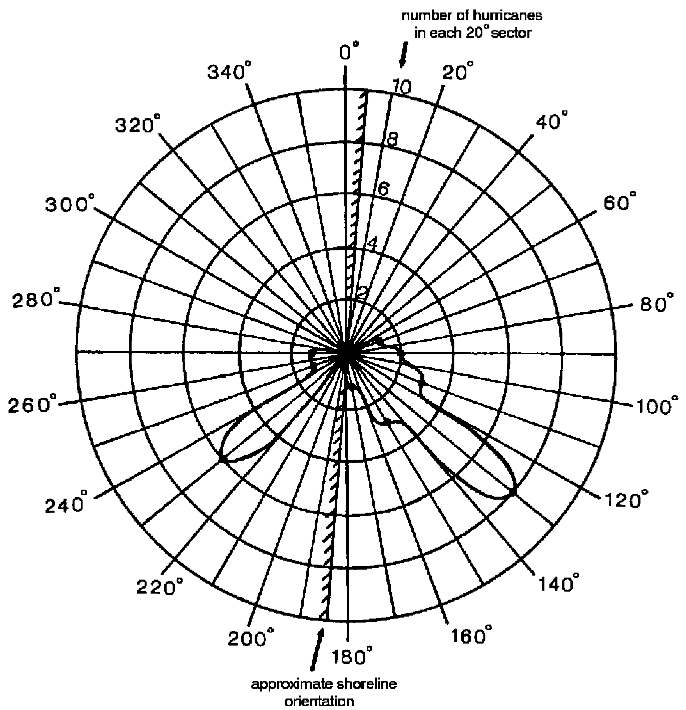

Figure 2 Direction Distribution of Historical Hurricanes in a 300 n.mi. Segment of Coast Comprising the Palm Beach Coastline

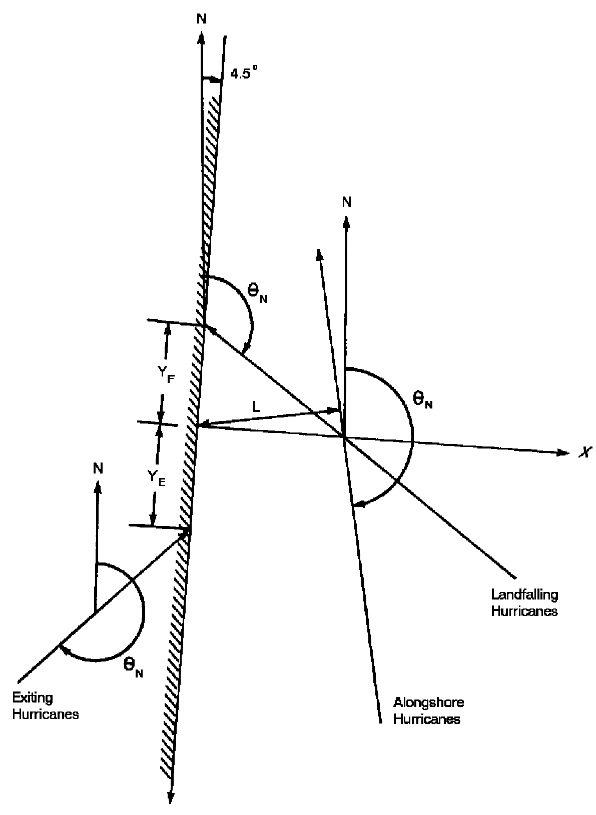

Figure 3 Definition Sketch of Three Types of Hurricanes

Based on historical data, it is expected that within a 2,000 year period a total of 591 hurricanes will occur within a distance of 300 n.mi. segment of the coast comprising the study area. Of the 591 hurricanes, 409 will be landfalling and 182 exiting.

For purposes of computer use, the cumulative probability distribution of hurricane track direction (θ_N) is developed from Figure 2 and is presented in Figure 5.

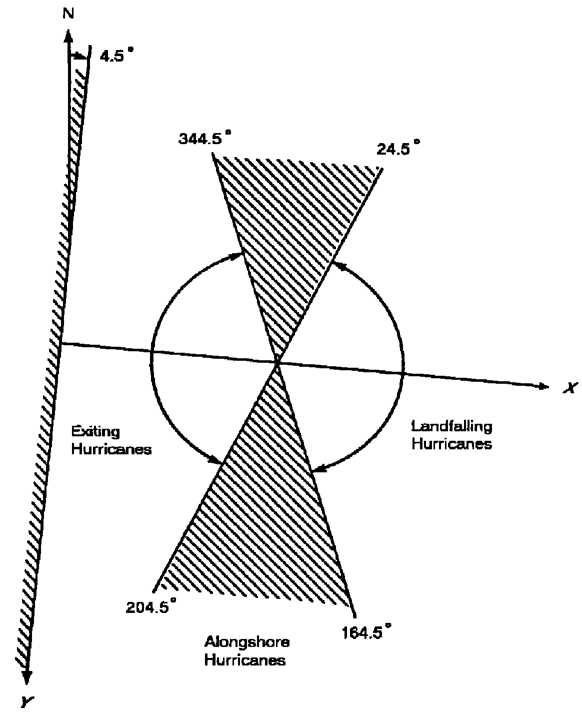

Figure 4 Designation of Landfalling, Alongshore, and Exiting Hurricanes for Palm Beach County Depending on Track Directions Relative to Shoreline Orientation

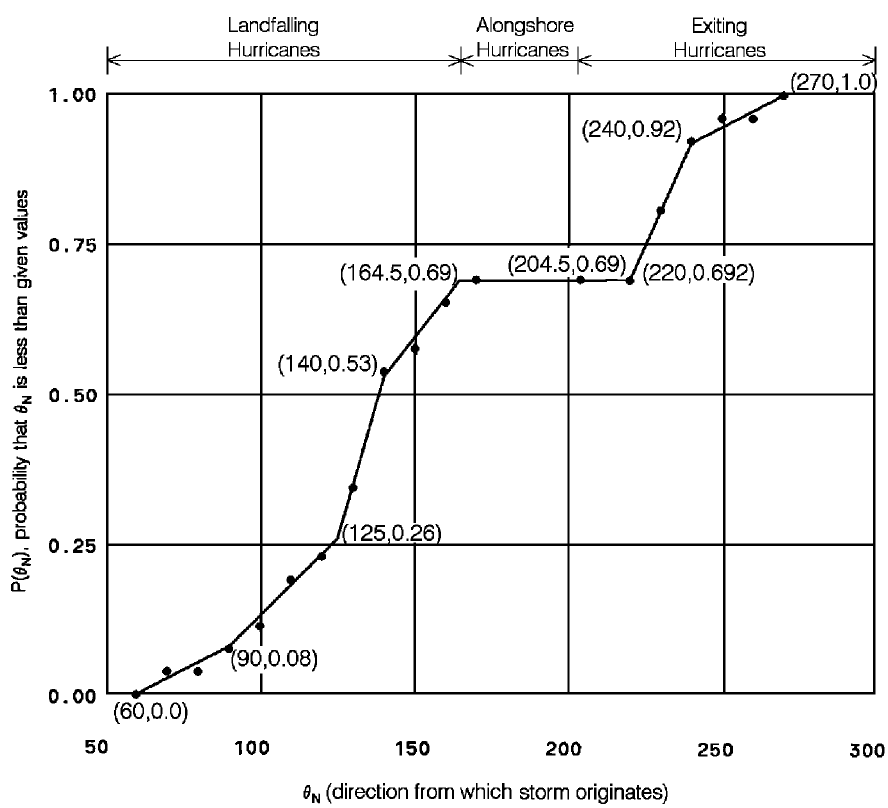

Figure 5 Cumulative Probability Distribution of Hurricane Track Direction, θ_N

2.3 Radius to Maximum Winds and Central Pressure Deficit

The cumulative probability distribution of radius to maximum winds for landfalling hurricanes is presented in Figure 6. Figure 7 presents the same for exiting hurricanes.

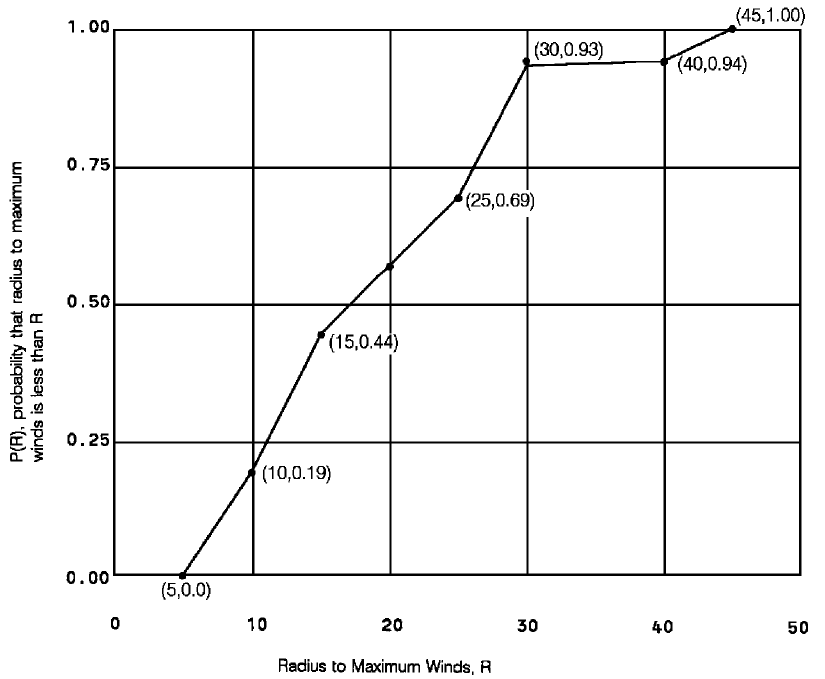

Figure 6 Cumulative Probability Distribution of Radius to Maximum Winds, R, for Landfalling Hurricanes

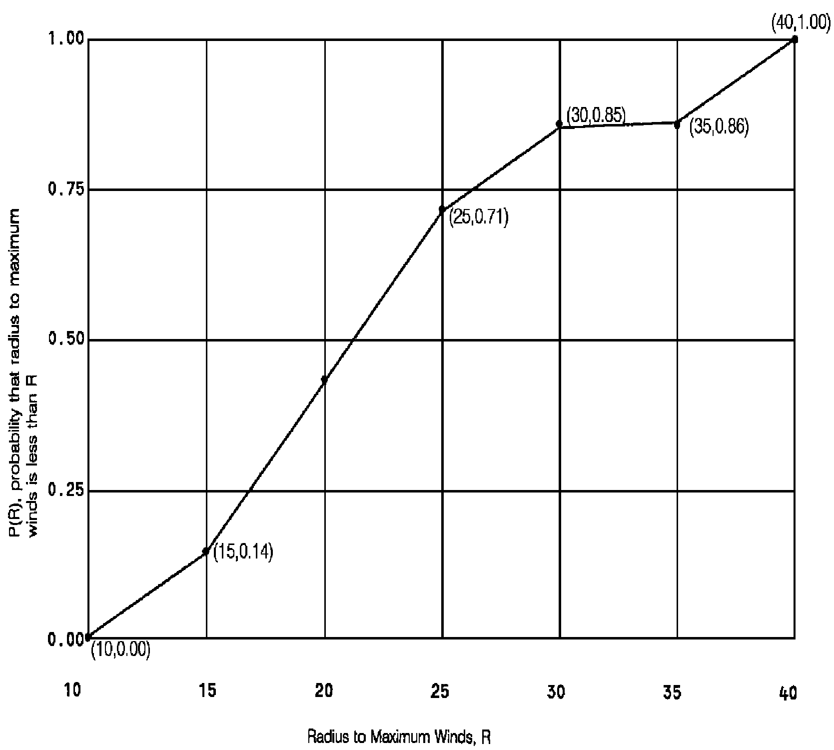

Figure 7 Cumulative Probability Distribution of Radius to Maximum Winds, R, for Exiting Hurricanes

The cumulative probability distribution of central pressure deficit for landfalling hurricanes is presented in Figure 8. Figure 9 presents the same for exiting hurricanes.

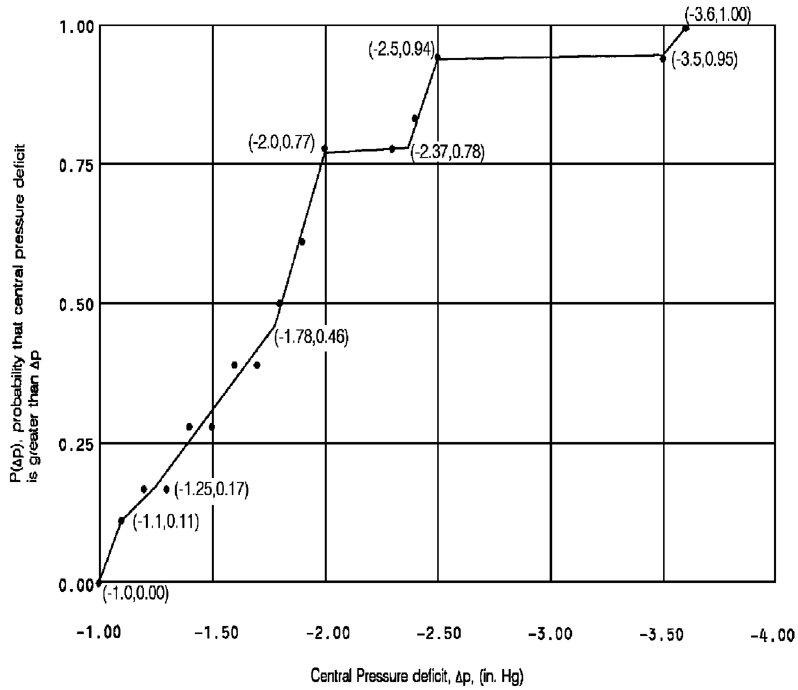

Figure 8 Cumulative Probability Distribution of Central Pressure Deficit, Δp, for Landfalling Hurricanes

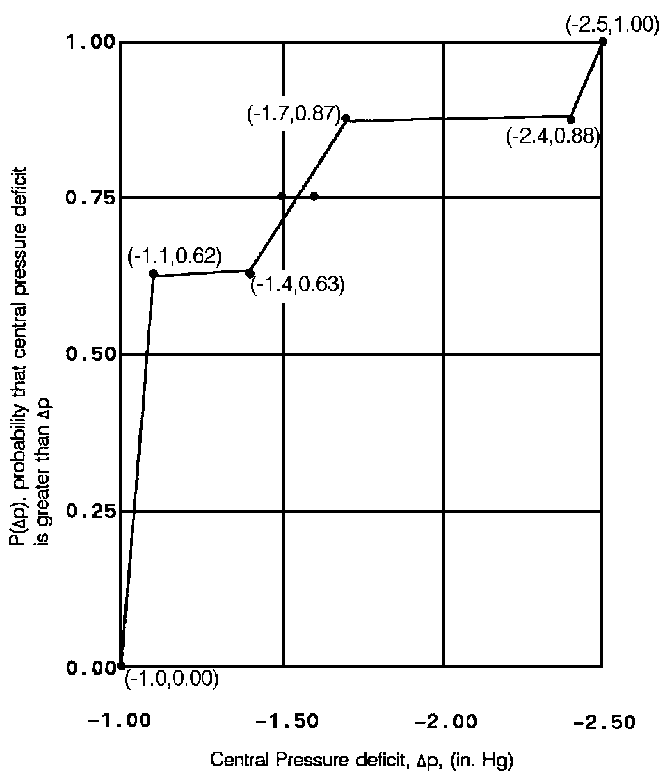

Figure 9 Cumulative Probability Distribution of Central Pressure Deficit, Δp, for Exiting Hurricanes

2.4 Forward Speed

The cumulative probability distribution of the forward speed of translation for landfalling hurricanes is presented in Figure 10. Figure 11 presents the forward speed of translation for exiting hurricanes.

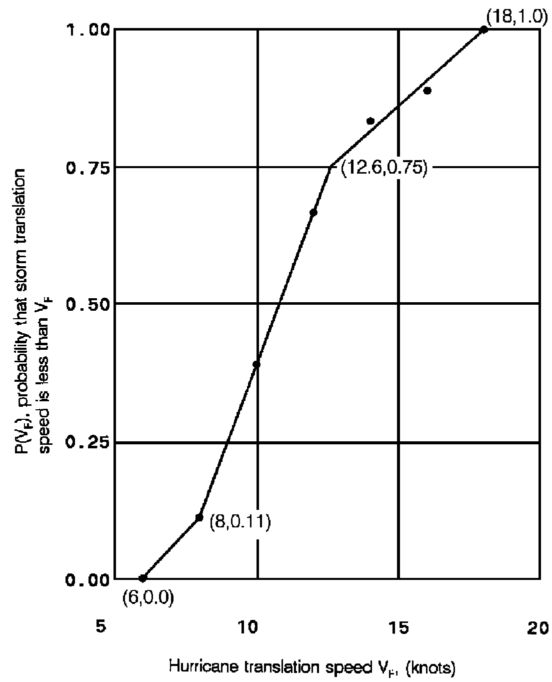

Figure 10 Cumulative Probability Distribution of Hurricane Translation Speed V_F, for Landfalling Hurricanes

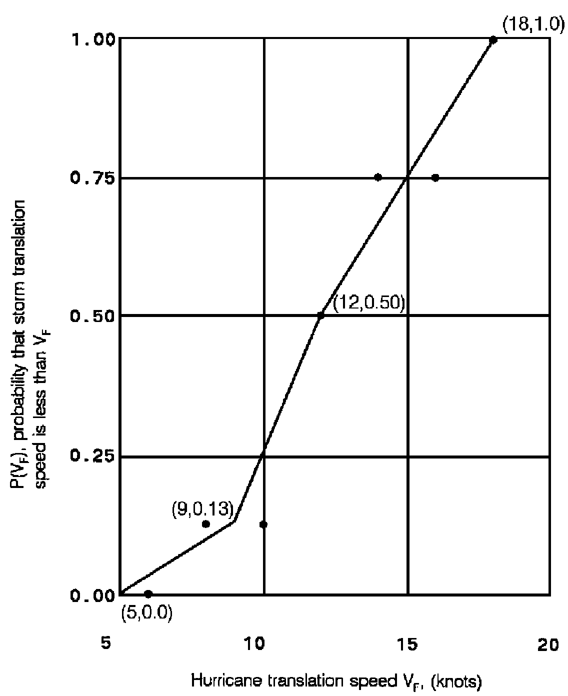

Figure 11 Cumulative Probability Distribution of Hurricane Translation Speed V_F, for Exiting Hurricanes

2.5 Track Position

For the landfalling and exiting hurricanes, the track position is determined by the y coordinate, Y_F and Y_E representing the landfalling and exiting point, respectively, as defined in Figure 3. Figure 12 presents the cumulative probability distribution for the actual landfalling position, Y_F, for landfalling hurricanes. Figure 13 presents the cumulative probability distribution for the actual landfalling position, Y_F, for exiting hurricanes.

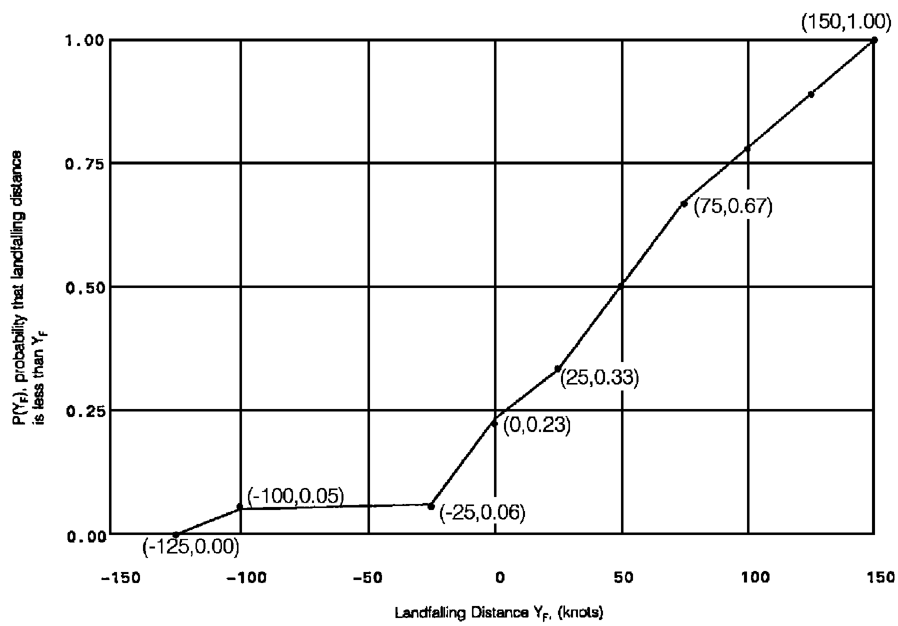

Figure 12 Cumulative Probability Distribution of Landfalling Distances, Y_F, for Landfalling Hurricanes

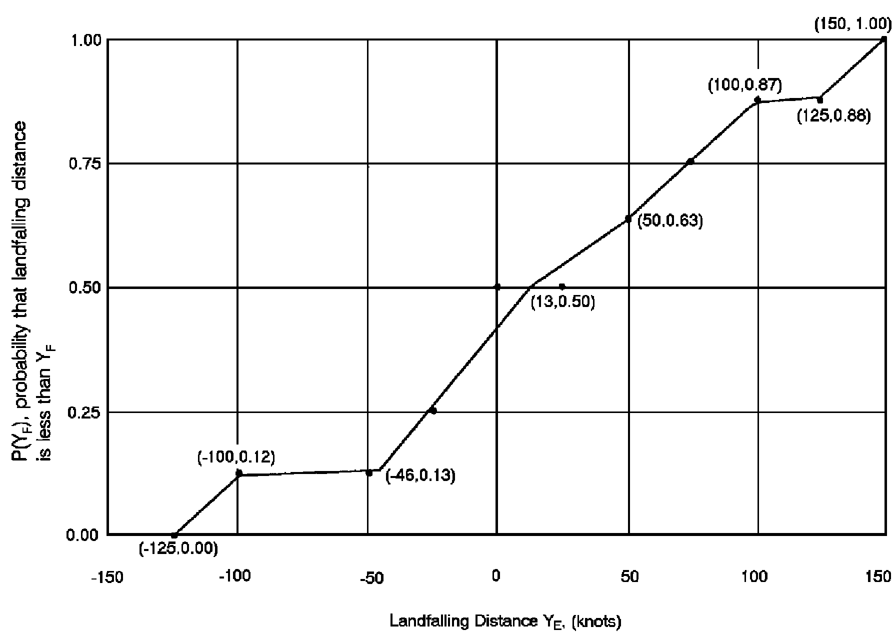

Figure 13 Cumulative Probability Distribution of Landfalling Distances, Y_E, for Exiting Hurricanes

III. METHODOLOGY

3.1 Introduction

This section describes the overall methodology at a very general level to provide the reader with an understanding of the general procedures without addressing the details. The objective of this study is to develop, verify and apply procedures which will yield valid estimates of the combined total storm tides associated with various return periods at the site of interest.

The approach used here is to combine the available historical statistics of hurricanes with a set of numerical models to simulate the storm tides at the site of interest. Figure 14 is a flow chart illustrating

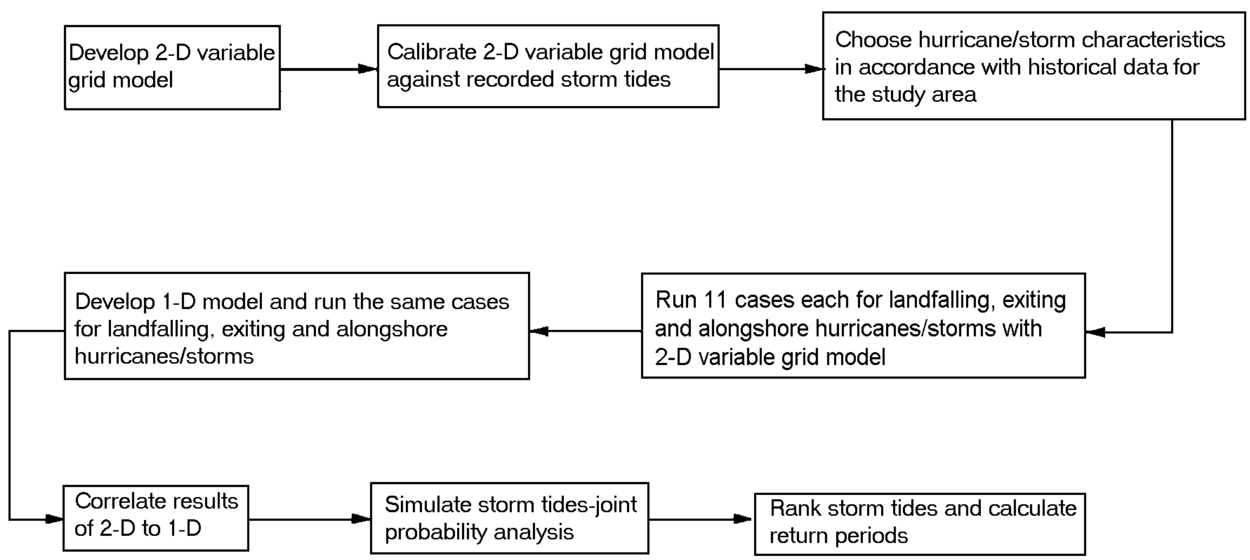

Figure 14 Flow Chart of Methodology

the overall procedure. The numerical models include two-dimensional the overall procedure. The numerical models include two-dimensional representations with a variable grid system for the offshore and coastal areas. Prior to its application, the model is verified using tide gage measurements during the hurricanes of 1926, 1945, 1947 and 1979. The two-dimensional model is significantly more expensive to operate and, because the simulation phase (which generates the statistics of the combined total storm tides) requires the computation of a few hundred hurricane events, a simpler, far less expensive one-dimensional model is developed and calibrated to yield reasonably good agreement with the predictions of the two-dimensional model. The following sections describe each of the elements in the overall calculation procedure.

3.2 Model Hurricane

The numerical models require, as input, some representation of the atmospheric pressures and winds which are responsible for the storm tide generation. For this purpose, a model hurricane is used that is characterized by the following five parameters:

Δp = Central Pressure Deficit

R = Radius to Maximum Winds

V_F = Speed of Hurricane System Translation

θ = Hurricane Direction

Y_F = Landfall location or some other descriptor of hurricane track.

The model hurricane is one proposed by Wilson (7) and is characterized by circular isobars. The associated wind field is determined from a solution of the governing equations of motion. The model hurricane is described in Appendix B.

3.3 Features of the Two-Dimensional Numerical Model

As noted previously, there is a variable grid two-dimensional model for the offshore and coastal areas which is used in the generation of storm tides for Palm Beach County. The grids of the model are arranged in such a way that

1) The finest grids cover the coastal areas of Palm Beach County to yield detailed information for the study. Fine grids are also used in locations where calibration of the model results against measured storm tides is to take place.
2) The coarsest grids cover the areas where detailed information is not needed.
3) A number of grids varying gradually in size are used for the transition from the coarsest to the finest grids and vice versa.

This arrangement of the varying grid system for the two-dimensional model gives good efficiency of computer time utilization.

The size of the finest grid is 1,000 ft. x 5,000 ft. and the coarsest 37,400 ft. x 44,800 ft. The two-dimensional model covers an area of 59.5 n.mi. x 152.9 n.mi. (77 x 92 grids) with the north-south orientation approximately parallel with the shoreline of Palm Beach County. Figure 15 shows the grid system layout.

The two-dimensional storm surge model is an implicit finite difference system in which the three governing differential equations are the two vertically averaged equations of momentum and the equation of continuity. The solution to the equations is carried out in a fractional time step procedure. The advantage of this fractional time step procedure is that it is time and space centered to the first order. The finite difference equations appropriate for implicit solution are

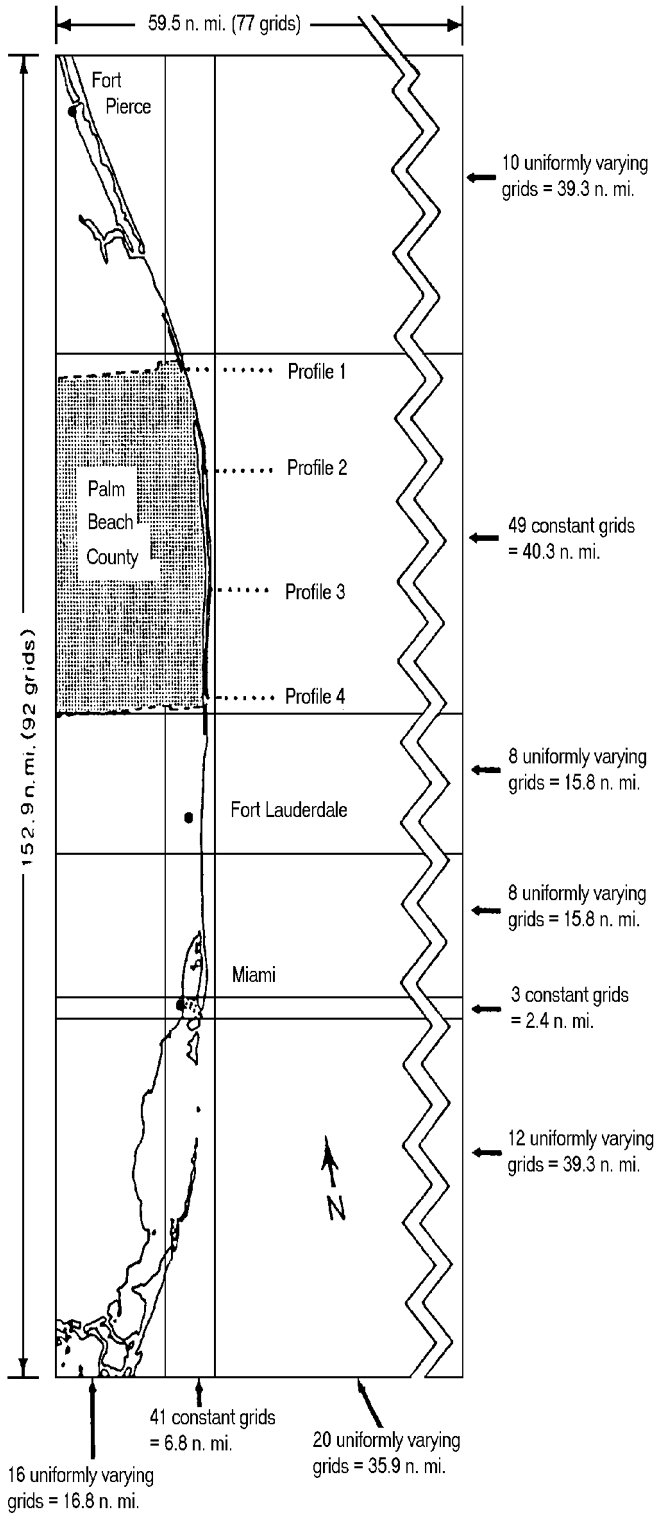

Figure 15 Grid System Layout for Palm Beach County

solved by the "double sweep" method, which is described in detail in Chapter IV. The surface (wind) and bottom (friction) shear stresses, the barometric pressure, the Coriolis effect, the components of slope of the water surface and the boundary conditions are all incorporated into the solution processes.

Inlets and barrier islands which are too small to be resolved by the normal grid sizes are represented in the model by a special treatment. The boundary conditions specified on the two-dimensional model are that the water surface displacement on the boundaries where water is present are equal to the barometric head, due to atmospheric pressure variations. The normal discharge at these boundaries is that necessary to satisfy the volume requirement by the rising and falling water surface encompassed by the boundaries. Although this is an approximation, if the boundaries are sufficiently distant from the site of interest, any extraneous effects of this approximation should be small. The second type of boundary condition is the no-flow requirement which ensures that the flows are zero normal to grid lines where land elevations exist that are higher than the adjacent water elevations. At times when the elevation of a rising water surface exceeds the land elevation of an adjacent grid block, that block is flooded by a simple algorithm and vice versa for the "deflooding" from grid blocks at times that the falling water surface leaves a block exposed. The effects of vegetation on bottom and surface friction factors are accounted for in an approximate manner.

3.4 Features of the One-Dimensional Numerical Model

As noted earlier, a simple one-dimensional numerical model was developed and calibrated to allow the statistics to be generated based on simulation (calculations) of many hurricanes and associated storm tides.

The one-dimensional numerical model is described as follows. A transect line is established which is approximately perpendicular to the bottom contours. The characteristics (Δp, R, θ_N, V_F and track) of the hurricane are defined and the hurricane is advanced along the track line. The water surface displacement (boundary condition) at the seaward end of the transect line is taken as the static response of the water surface to the barometric pressure deviation at that point. The locations of the four transect lines (profiles) for Palm Beach County are shown in Figure 15. Figures 16a, 16b, 16c and 16d present the profiles of the four transect lines and their one-dimensional grid representations.

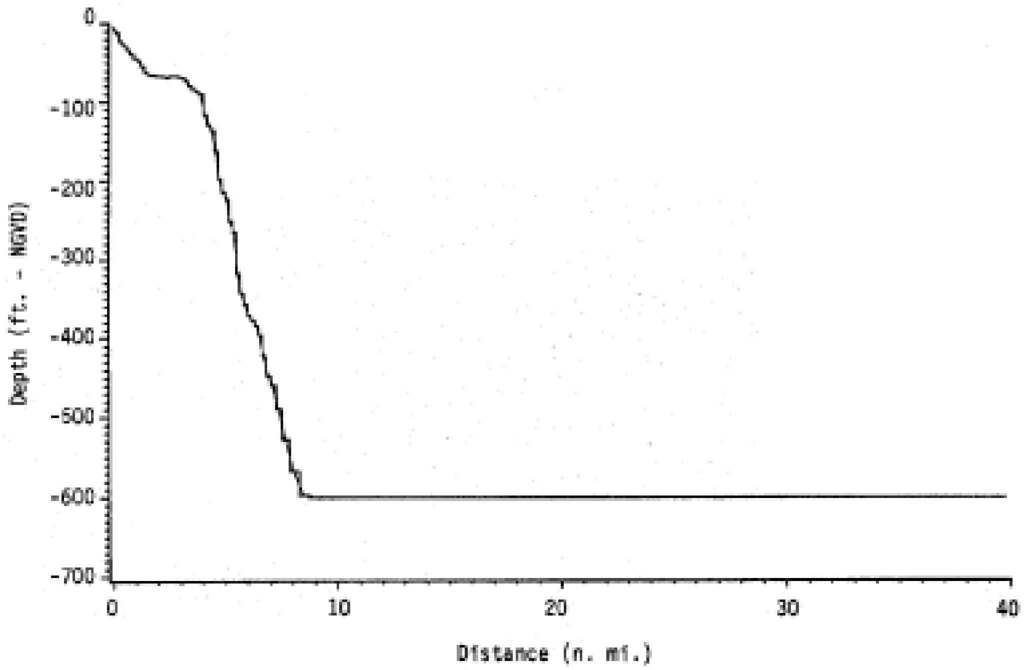

Figure 16a   Profile One Transect Line and Its One-Dimensional Grid Representation

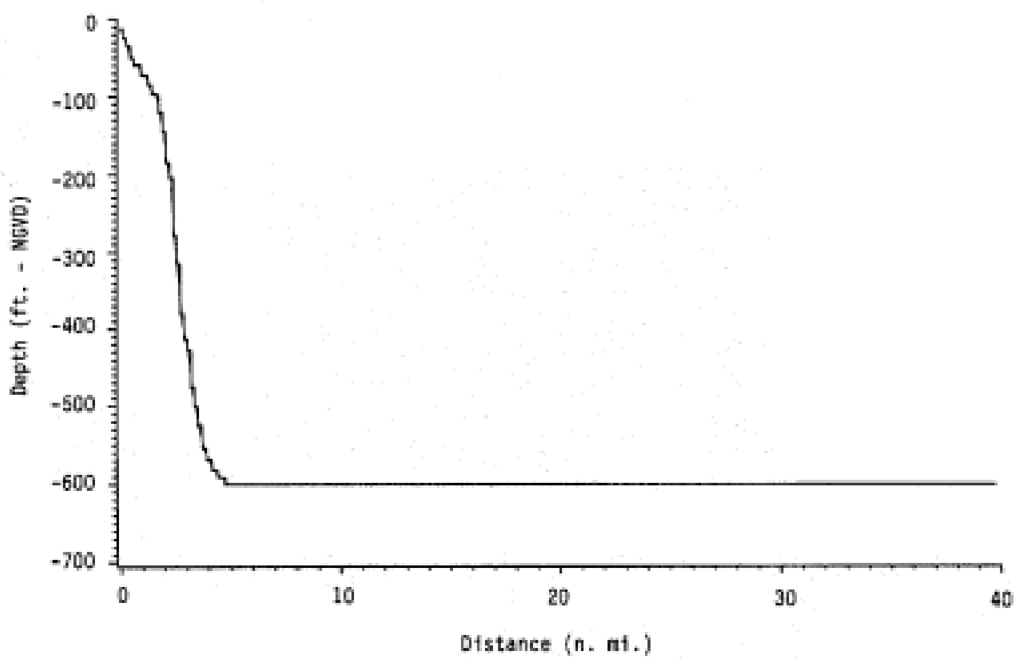

Figure 16b   Profile Two Transect Line and Its One-Dimensional Grid Representation

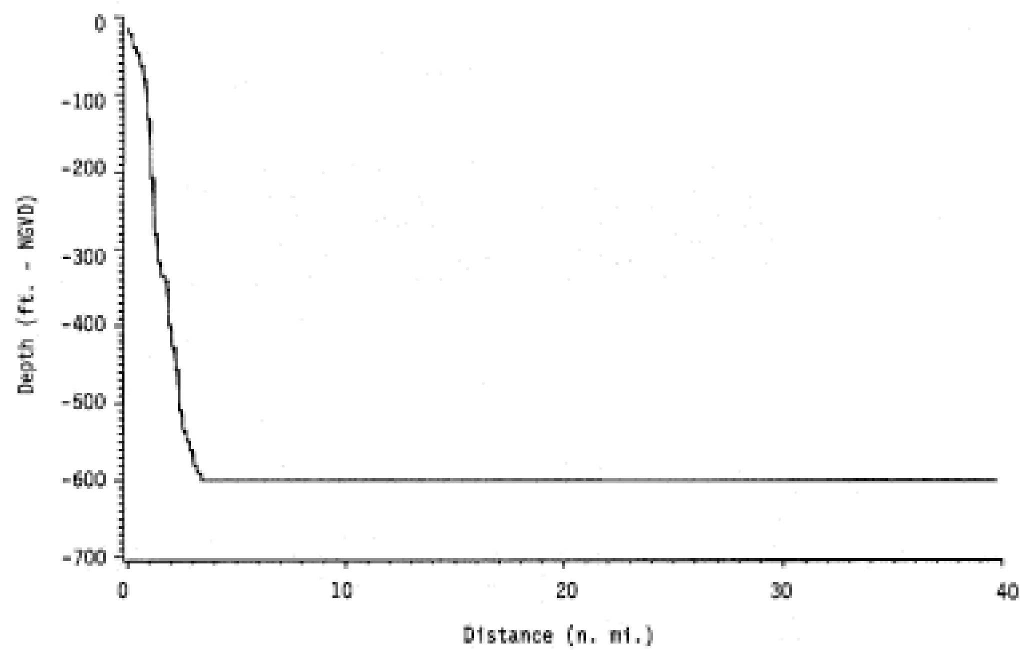

Figure 16c   Profile Three Transect Line and Its One-Dimensional Grid Representation

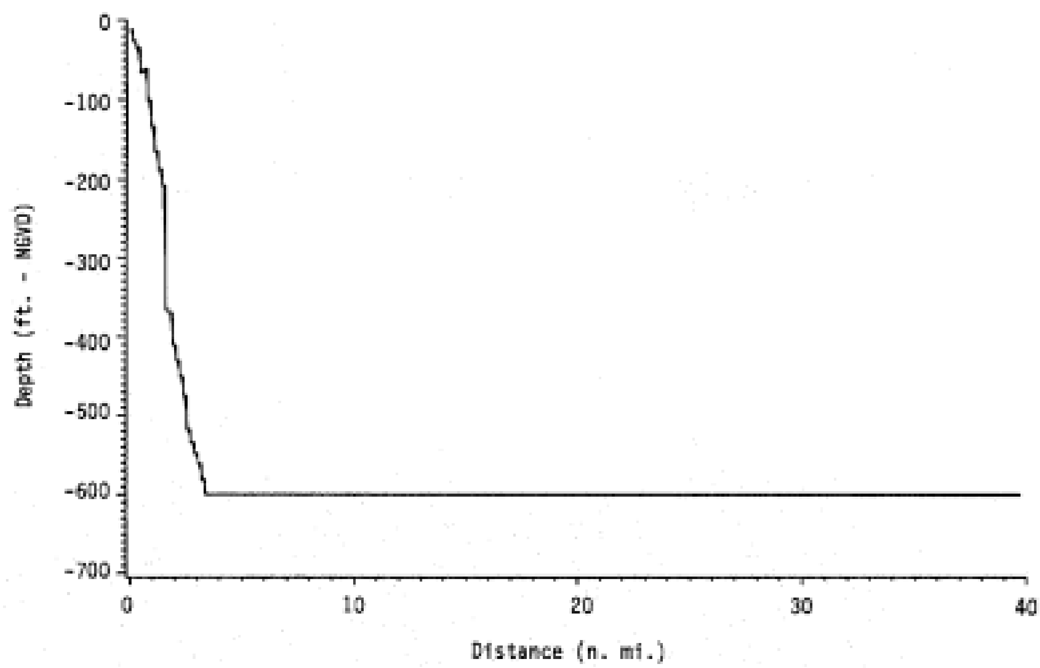

Figure 16d   Profile Four Transect Line and Its One-Dimensional Grid Representation

3.5 Application of Numerical Models

The numerical models are applied in the following different phases:

1) Verifications of the two-dimensional numerical model against tide gage recordings of the September 1926, 1945, 1947 and 1979 hurricanes.
2) Based on the characteristics of historical hurricanes, the two-dimensional model is run for 11 cases of landfalling, alongshore and exiting hurricanes with characteristics representative of the more probable and significant hurricanes.
3) The one-dimensional model is run for the same 11 cases for each type of hurricanes described in 2) above. The storm tides developed in 2) then serve as a basis for adjusting the output of the one-dimensional model during the simulation phase.

3.6 Simulation of a n-Year Sequence of Hurricane Associated Storm Tides

With the statistical characteristics of historical hurricanes available and the simple one-dimensional model calibrated as described in the preceding section, the simulation shown in Figure 17 is carried out. The first phase of the simulation comprises the selection of the hurricane characteristics in accordance with the historical data. In each hurricane, this involves the following:

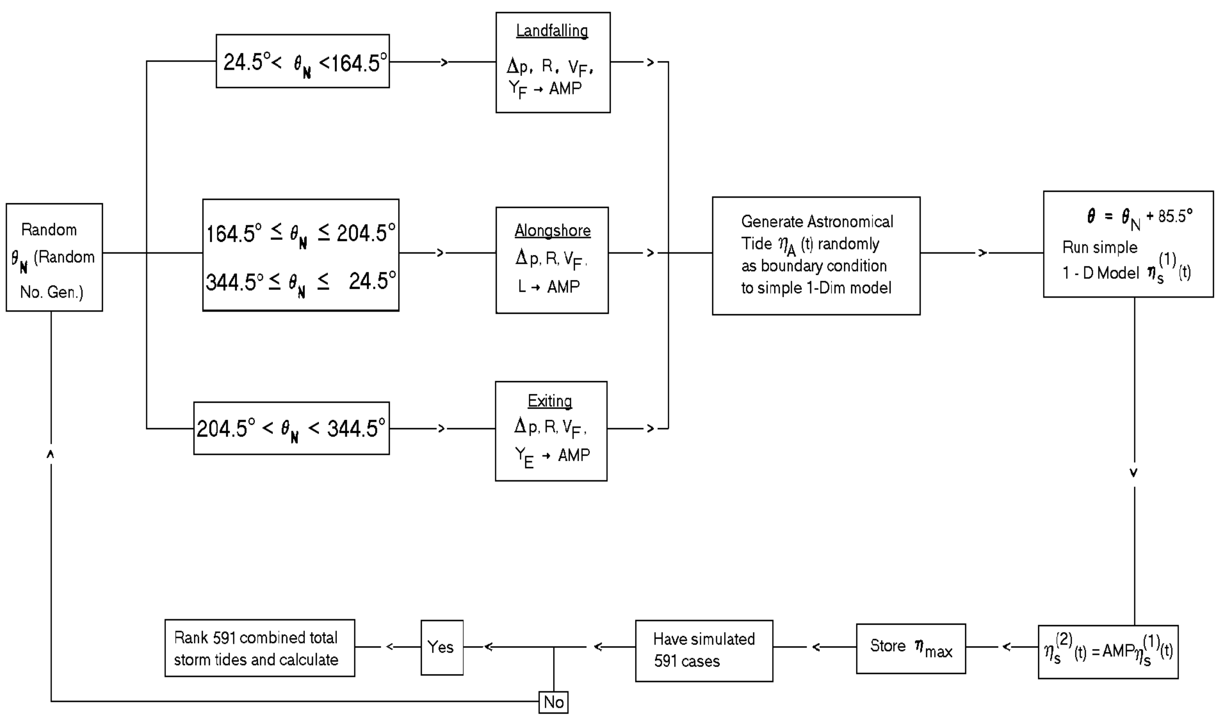

Figure 17 Flow Chart for Storm Tide Simulations Using One-Dimensional Model (after Calibration with Two-Dimensional Model)

1) Quantifying Δp, R, V_F, Θ_N and hurricane track in accordance with the historical probabilities.
2) For these characteristics, a random astronomical tide from the hurricane season is generated as a boundary condition to the one-dimensional numerical model and the model is run to determine the storm surge at the site of interest. This storm surge with dynamic wave set up is then adjusted in

accordance with the factors obtained from the two-dimensional model calibration runs for the landward grid at each time step to yield the combined total storm tide.

3) Determining whether enough hurricanes have been simulated for the n-year simulation.

4) After the required number of hurricanes and associated storm tides have been simulated, the peak water levels for each hurricane are ranked and the return period, TR, is calculated, according to

$$TR = 2000/M$$

where M is the rank of the combined total storm tide level. (For example, if the simulation was carried out for a 2,000 year period, the highest combined total tide level would have a return period of 2,000 years, the fourth highest water level would have a return period of 500 years, etc.). Finally, by presenting these results on semi-log paper, it is possible to interpolate the return periods of interest, i.e., TR = 5, 10, 20, 50, 100, 200 and 500 years, to yield the final results for the present study.

IV. NUMERICAL MODELS-DESCRIPTION AND CALIBRATION

As noted in the previous chapter the methodology included the development, calibration and application of a series of numerical models and statistical hurricane characteristics to the simulation of a long period (2,000 years) to establish storm water levels associated with various return periods of interest. Figure 14 presents a flow chart of the methodology. This chapter parallels that of Chapter III; however, much greater detail is presented. The following subsections review the various numerical models and calibration or calculation procedures.

4.1 Two-Dimensional Numerical Model

Variable-Grid Two-Dimensional Numerical Model - The grid associated with this numerical model relative to the shoreline is presented in Figure 15. The coarsest grid of the model is 6.16 n.mi. x 7.37 n.mi. and the finest is 0.16 n.mi. x 0.82 n.mi. and the purpose of the numerical model is to calculate the storm tides as the storm translates across the shelf.

Governing Differential Equations - The governing differential equations for the two-dimensional model are the two vertically averaged equations of momentum and the equation of continuity, break given by:

Momentum Equations

$$\frac{\partial q_x}{\partial t} + \frac{q_x}{D}\frac{\partial q_x}{\partial x} + \frac{q_y}{D}\frac{\partial q_x}{\partial y} = gD\frac{\partial \eta}{\partial x} - \frac{D}{p}\frac{\partial p}{\partial x} + \frac{\tau_{w_x}}{\rho} - \frac{\tau_{w_x}}{\rho} - \beta q_y \qquad (1)$$

$$\frac{\partial q_y}{\partial t} + \frac{q_x}{D}\frac{\partial q_y}{\partial x} + \frac{q_y}{D}\frac{\partial q_y}{\partial y} = gD\frac{\partial \eta}{\partial y} - \frac{D}{p}\frac{\partial p}{\partial y} + \frac{\tau_{w_y}}{\rho} - \frac{\tau_{w_y}}{\rho} + \beta q_x \qquad (2)$$

Continuity Equation

$$\frac{\partial \eta}{\partial t} + \frac{\partial q_x}{\partial x} + \frac{\partial q_y}{\partial y} = 0 \qquad (3)$$

in which

q_x = volumetric transport component per unit width in the *x* direction

q_y = volumetric transport component per unit width in the *y* direction

t = time

D = total water depth (h + η) including the still water depth, h and the storm surge, η

η	=	storm surge above mean water level
x	=	horizontal coordinate, directed offshore
y	=	horizontal coordinate direction according to the left-hand coordinate system
g	=	gravitational constant
ρ	=	mass density of water
p	=	barometric pressure
τ_{w_x}	=	wind shear stress component in the *x* direction
τ_{w_y}	=	wind shear stress component in the *y* direction
τ_{b_x}	=	wind shear stress component in the *x* direction
τ_{b_y}	=	wind shear stress component in the *y* direction
f	=	Darcy-Weisbach friction coefficient
β	=	Coriolis parameter = $2\Omega \sin\psi$
Ω	=	angular speed of earth rotation = 7.27 x 10^{-5} rad/sec
ψ	=	latitude of site of interest

The surface and bottom shear stress components are related to the wind speed *W* and discharge components by:

$$\tau_{w_x} = \rho K W W_x \quad \text{and} \quad \tau_{w_y} = \rho K W W_y \tag{4}$$

$$\tau_{b_x} = \frac{\rho f\,|q|\,q_x}{8D^2} \quad , \quad \tau_{b_y} = \frac{\rho f\,|q|\,q_x}{8D^2} \quad \text{where}\,|q| = \sqrt{q_x^2 + q_y^2} \tag{5}$$

in which *K* is an air-sea friction coefficient developed by Van Dorn (8); and depends on the wind speed, *W*, as follows:

$$K = \begin{cases} 1.1x10^{-6} & \text{for } W < W_{cr} \\ 1.1x10^{-6} + 2.5\ x\ 10^{-6}(1 - W_{cr}/W)^2 & \text{for } W \geq W_{cr} \end{cases} \tag{6}$$

where W_{cr} = 23.6 ft/sec.

The quantity, *f*, is the Darcy-Weisbach bottom friction coefficient and varies with depth, bottom roughness and vegetation, if present. For purposes of this study, *f* was developed by Christensen and Walton (9) of the University of Florida and is presented in Figure 18.

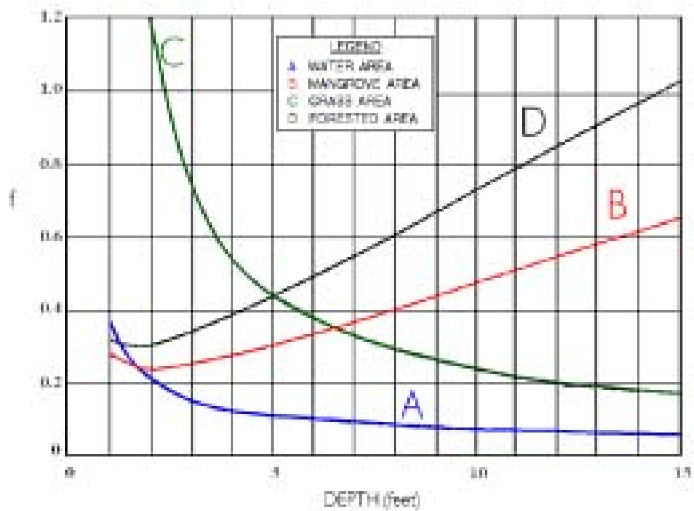

Figure 18 Bottom Friction Coefficients for Various Bottom Conditions

Finite Difference Forms of Governing Differential Equations - The finite difference representations of Equations (1) and (2) are expressed as follows with the convective terms $\left(i.e.\frac{q_x}{D}\frac{\partial q_x}{\partial x}, etc.\right)$ omitted in preparation for an implicit type of solution. The solution to the equations will be carried out in a fractional time step procedure. This procedure is schematized in Figure 19. The advantage of this fractional time step procedure is that it is time and space centered to first order.

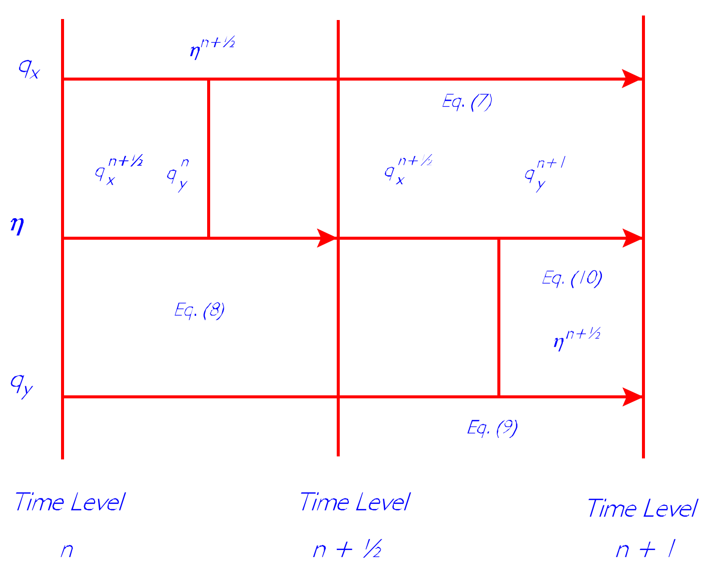

Notes: (1) Vertical links denote equations which are solved simultaneously.
(2) Values adjacent to the horizontal bars indicate the time level of the different variables entering into the computations.

Figure 19 Schematic of Implicit Method of Solving Momentum and Continuity Equations

The finite difference equations for the first portion of the fractional time step that are appropriate for the implicit method of solution are:

$$\mathrm{A_i}\,\eta_{i,j}^{\mathrm{n+1/2}} + \mathrm{B_i}\,q_{x_{i,j}}^{\mathrm{n+1}} + \mathrm{C_i}\,\eta_{\mathrm{i,j}}^{\mathrm{n+1/2}} = \mathrm{D_i} \qquad (7)$$

$$\mathrm{A_i^*}\,q_{x_{i+1,j}}^{n+1} + \mathrm{B_i^*}\,\eta_{i,j}^{\mathrm{n+1/2}} + \mathrm{C_i^*}\,q_{x_{i,j}}^{n+1} = \mathrm{D_i^*} \qquad (8)$$

where Equation (7) represents the momentum equation in the x-direction and Equation (8) represents the continuity equation; these two equations are to be solved simultaneously. The second set of simultaneous equations representing flow in the y-direction which is solved subsequent to the solution of the first set is:

$$\mathrm{A_j}\,\eta_{i,j}^{\mathrm{n+1}} + \mathrm{B_j}\,q_{x_{i,j}}^{\mathrm{n+1}} + \mathrm{C_j}\,\eta_{\mathrm{i,j-1}}^{\mathrm{n+1}} = \mathrm{D_j} \qquad (9)$$

$$\mathrm{A_j^*}\,q_{y_{i,j+1}}^{n+1} + \mathrm{B_j^*}\,\eta_{i,j}^{\mathrm{n+1/2}} + \mathrm{C_j^*}\,q_{y_{i,j}}^{n+1} = \mathrm{D_j^*} \qquad (10)$$

<u>Implicit Solution of the Finite Difference Equations</u> - The solution for each time step progresses by first solving Equations (7) and (8) simultaneously for each *j* grid line sweeping over all values of *i*. This establishes the values of $\eta^{n+1/2}$ and q_x^{n+1} for the entire *(i,j)* field. The procedure is then repeated for Equations (9) and (10) in which this pair of equations is solved simultaneously for η^{n+1} and q_y^{n+1} for the entire (*i,j*) field. This latter pair of equations is expressed sequentially for each value of i, then solved for all values of *j*, for that particular *i* grid line. The expressions for the various coefficients are presented as follows.

$$A_i = g\overline{(h+\eta)}\,\frac{\Delta t}{\Delta x}$$

$$B_i = 1 + \frac{\mathrm{f}\,|q_{i,j}^{n}|\,\Delta t}{g(h+\eta)^2}$$

$$C_i = A_i$$

$$D_i = q_{x_{i,j}}^{n} + \Delta t\left[-\frac{\overline{(h+\eta)}}{\rho}\frac{\partial p}{\partial x} + \frac{\tau_{w_{x_{i,j}}}}{\rho} - \beta(\bar{q}_{y_{i,j}})^n\right]$$

$$A_i^* = \frac{\Delta t}{4\Delta x}$$

$$B_i^* = 1.0$$

$$C_i^* = -\frac{\Delta t}{4\Delta x}$$

$$D_i^* = \eta_{i,j}^n - \frac{\Delta t}{4\Delta x}(q_{x_{i+1,j}}^n - q_{x_{i,j}}^n) - \frac{\Delta t}{2\Delta y}(q_{y_{i,j+1}}^n - q_{y_{i,j}}^n)$$

$$\overline{q}_{y_{i,j}}^n = \frac{1}{4}\left[q_{y_{i-1,j}}^n + q_{y_{i,j}}^n + q_{y_{i-1,j+1}}^n + q_{y_{i,j-1}}^n\right]$$

$$|q_{i,j}^n| = \sqrt{(q_{y_{i,j}}^n)^2 + (\overline{q}_{x_{i,j}}^n)^2} \qquad \text{(To be used in expression } \mathrm{B_i}\text{)}$$

$$A_j = \frac{g\overline{(h+\eta)}}{2}\frac{\Delta t}{\Delta y}$$

$$B_j = 1 + \frac{\mathrm{f}\,|q_{i,j}^n|\,\Delta t}{g(h+\eta)^2}$$

$$C_j = A_j$$

$$D_j = q_{y_{i,j}}^n + \Delta t\left[-g\frac{\overline{(h+\eta)}}{2}\frac{\Delta t}{\Delta y}(\eta_{i,j}^n - \eta_{i,j-1}^n) - \frac{\overline{(h+\eta)}}{\rho}\frac{\partial p}{\partial y} + \frac{\tau_{w_{y_{i,j}}}}{\rho} + \beta(\overline{q_{x_{i,j}}})^n\right]$$

$$\overline{q}_{x_{i,j}}^n = \frac{1}{4}\left[q_{x_{i-1,j}}^n + q_{x_{i,j-1}}^n + q_{x_{i+1,j}}^n + q_{x_{i+1,j-1}}^n\right]$$

$$|q_{i,j}^n| = \sqrt{(\overline{q}_{x_{i,j}}^n)^2 + (q_{y_{i,j}}^n)^2} \qquad \text{(To be used in expression } \mathrm{B_j}\text{)}$$

$$A_j^* = \frac{\Delta t}{4\Delta y}$$

$$B_j^* = 1.0$$

$$C_j^* = -A_j^*$$

$$D_j^* = \eta_{i,j}^{n+1/2} - \frac{\Delta t}{4\Delta x}(q_{x_{i+1,j}}^n - q_{x_{i,j}}^n) - \frac{\Delta t}{4\Delta y}(q_{x_{i+1,j}}^{n+1} - q_{x_{i,j}}^{n+1}) - \frac{\Delta t}{4\Delta x}(q_{y_{i,j+1}}^n - q_{y_{i,j}}^n)$$

With the coefficients now specified, the method of solving the sets of simultaneous equations will be described. The method is termed the "doubled sweep" method in which the first sweep involves "conditioning" two sets of auxiliary coefficients (E_i, F_i, E_i^*, F_i^*). The second sweep determines the values of η and *q* and, in the process, incorporates the required boundary conditions. The procedure will be illustrated for Equations (7) and (8) and it is noted that the same procedure is applicable to solving Equations (9) and (10). The procedure commences by establishing two auxiliary equations with four variables *(E_i, F_i, E_i^*, F_i^*)*.which are initially unknown,

$$\eta_{i,j}^{n+1/2} = E_i \; q_{x_{i,j}}^{n+1} + F_i \tag{11}$$

$$q_{x_{i+1,j}}^{n+1} = E_i^* \eta_{i,j}^{n+1/2} + F_i^* \tag{12}$$

Equations (11) and (12) are substituted in Equations (7) and (8) and the results simplified to yield

$$q_{x_{i,j}}^{n+1} = - \frac{C_i}{A_i E_i + B_i} \eta_{i-1,j}^{n+1/2} + \frac{D_{i\,-}\; A_i F_i}{A_i E_i + B_i} \tag{13}$$

$$\eta_{i,j}^{n+1/2} = - \frac{C_i^*}{A_i^* E_i^* + B_i^*} q_{x_{i,j}}^{n+1} + \frac{D_i^* - A_i^* F_i^*}{A_i^* E_i^* + B_i^*} \tag{14}$$

Comparison of Equations (13) and (14) establishes the values of the unknown coefficients in terms of the known coefficients *(E_i, F_i, E_i^*, F_i^*)* .(*A, B, ..., A*, B*,...*). The expressions are

$$E_i = - \frac{C_i^*}{A_i^* E_i^* + B_i^*} \quad , \quad F_i = \frac{D_i^* - A_i^* F_i^*}{A_i^* E_i^* + B_i^*} \tag{15}$$

$$E_{i-1}^* = - \frac{C_i}{A_i E_i + B_i} \quad , \quad F_{i-1}^* \frac{D_i \; - A_i F_i}{A_i E_i + B_i} \tag{16}$$

To illustrate the manner in which boundary condition information is incorporated into the procedure, suppose that the water surface level, η, is specified at *i = IMAX* and that q_x is specified as zero at i = 2[˜]. The first sweep commences by noting (from Equation 11) that

$$\begin{aligned} E_{IMAX} &= 0.0 \\ F_{IMAX} &= \eta^{n+1/2}_{IMAX,j} \end{aligned} \tag{17}$$

With the values of E_{IMAX} and F_{IMAX} now known, E^*_{IMAX-1} and F^*_{IMAX-1} can be calculated from Equations (16), then values of E_{IMAX-1} and F_{IMAX-1} computed from Equations (15) and so on. E^*_i and F^*_i are set equal to

$$\begin{aligned} E^*_i &= 0.0 \\ F^*_i &= 0.0 \end{aligned} \tag{18}$$

in accordance with the boundary condition and Equation (12). This completes the first sweep and establishes all the coefficients over the grid line.

The second sweep simply consists of applying the methodology to the y-direction as described in detail for the x-direction. In summary, the "double sweep" procedure as presented here progresses from large i to small i for the first sweep and then progresses back from small i to large i for the second sweep.

It can be shown that this procedure results in an exact solution of the tridiagonal set of simultaneous equations represented by Equations (7) and (8). As noted previously the same procedure is then applied to solve Equations (9) and (10) which completes establishing η, q_x, and q_y at the ($n+1$) time step.

4.2 Boundary Conditions

To complete formulation of the problem, boundary conditions must be specified at the boundaries of the grid presented in Figure 15. On the "open" (water) boundaries, the water surface, $\eta_{B_{i,j}}$, is specified to be that associated with the barometric pressure, i.e.,

$$\eta_{B_{i,j}} = \left(\frac{p_\infty - p_{i,j}}{\rho g} \right) \tag{19}$$

in which p_∞ denotes the far field barometric pressure. In addition, on the open boundary grid cells, it is specified that only discharge components perpendicular to the boundaries occur and that these discharges on the exterior boundaries of the grid system are those required to satisfy the continuity equation (Equation 3). On the "closed" boundaries, i.e., at the shoreline where land elevations are higher than the

---

[˜]It is noted that other combinations of boundary conditions at the two ends for the grid line could be accommodated. Also, internal boundary conditions of the type $q^{n+1}_{x_{i,j}} = 0$ are satisfied by the choice of coefficients: $E^*_{i-1} = F^*_{i-1} = 0$.

adjacent water elevations, a no-flow boundary condition is specified perpendicular to that boundary. However, "flooding" and "deflooding" of grid blocks adjacent to the boundaries can occur. Flooding occurs when the water level is greater by a specified small amount than the ground elevation of an adjacent grid block. When this condition exists, the grid block is activated by a simple allocation of this excess elevation on the newly activated block and in subsequent time steps the grid block is incorporated into the normal calculation scheme. Deflooding occurs when the water level on a grid block drops below a specified level leaving a very small depth on that block. The block is "deactivated" and the excess water placed on the adjacent grid.

The solution is started from an initial condition of zero water surface displacement and zero discharge components. The hurricane system is translated along a specified path at a designated speed. At each time step, the hurricane effects (represented by the pressure and wind stress components) on each cell are calculated and the finite-difference equations (Equations 7, 8, 9, and 10) employed. The results are updated values of η, q_x and q_y for each cell.

4.3 <u>One-Dimensional Numerical Model</u>

The one-dimensional numerical model is significantly less expensive, faster and simpler to run and is used in the simulation phase, in order to generate the required data within budgetary constraints. The justification for using the one-dimensional model is that it can be adequately calibrated with the rather complete two-dimensional model.

The one-dimensional numerical model is a static model with the exception of the Coriolis term for which the effects of inertia are included. The finite difference forms of the governing one-dimensional differential equations are (10):

$$\eta_{i+1}^{n+1} = \eta_i^{n+1} + \frac{\Delta x}{g(\overline{\overline{h+\eta}})}\left[\frac{\tau_{w_{x_i}}}{\rho} - \beta\, q_{y_i}^{n+1}\right] + \frac{p_i^{n+1} - p_{i+1}^{n+1}}{\rho g} \qquad (20)$$

$$q_{y_i}^{n+1} = \frac{1}{BB}\left[q_{y_i}^{n} + \frac{\Delta t}{\rho}\tau_{w_{y_i}}\right] \qquad (21)$$

where

$$BB = 1.0 + \frac{f\Delta t\,|q_{y_i}^{n}|}{8(\overline{\overline{h+\eta}})^2}$$

and the remaining variables are as defined previously for the two-dimensional model.

The one-dimensional model is initiated from a condition of rest (q_y = 0) and zero water surface displacement (η = 0). The only boundary condition required is that at the seaward end (i = 1) of each transect where the "barometric tide" is imposed as

$$\eta_1 = \frac{p_\infty - p_1}{\rho g} \tag{22}$$

In applying the one-dimensional numerical model, a variable grid size (1,000 ft. to 60,000 ft.) is used as presented in Figures 16a, 16b, 16c and 16d.

4.4 Simulation

To summarize information presented earlier, this phase includes the simulation of the occurrence of 2,000 years of hurricanes along a shoreline segment of 300 n.mi. The simulated hurricanes include landfalling, alongshore and exiting hurricanes with directional distributions according to Figure 5. In an average 2,000 year period, there would be a total of 591 hurricanes.

Selection of Hurricane Parameters - Each of the five idealized hurricane parameters [Radius to Maximum Winds, R; Central Pressure, p_o (or Central Pressure Deficit, Δp); Track Direction, θ_N; System Forward Speed, V_F; and Track Position] is determined randomly in accordance with the associated cumulative probability distribution functions. The procedure is described below for the track direction, θ_N, and is similar for all other variables.

The approximate piece-wise linear cumulative probability distribution function for track direction, θ_N, is shown in Figure 5. The nature of this function is such that the more predominant directions are those where the function rises steeply. To randomly select a track direction in accordance with the distribution function, the computer first generates a random number between 0 and 1 corresponding to the cumulative probability. Suppose that this number is 0.50. Since this value corresponds to the linear segment between directions of 125.0° and 140.0°, the computer interpolates to find a track direction, θ_N, of 138.33°. We note that this is a landfalling hurricane. The other four parameters are determined similarly with a separate and independent random number being generated for each parameter and the appropriate cumulative probability distribution used.

Calculation of Storm Surge with the Effect of Astronomical Tide - A particular hurricane can be "phased" such that the maximum resulting storm surge is increased or decreased by astronomical tidal fluctuations. Considering the predicted ocean astronomical tidal fluctuations at Lake Worth, Atlantic Ocean from June 1 to November 30, 1984 to be representative of those occurring during the hurricane season and assuming the phasing of hurricane occurrence and astronomical tides to be independent, the combination of these tidal components is carried out in the following manner.

With the hurricane parameters established, a starting time for the hurricane is selected randomly between June 1 and November 30, 1984. The corresponding astronomical tide at the starting time is generated as the boundary condition in the one-dimensional model and varies with time thereafter according to the input astronomical tide data. The calculation of the storm surge history by the calibrated one-dimensional model is thus phased with the astronomical tide to yield the combined storm surge and astronomical tide water level history at the site of interest.

Dynamic Wave Set-Up - When waves break, a shoreward directed force in addition to the wind stress, is exerted on the water in the surf zone. This causes an additional rise in water level termed "wave set-up". This effect has been studied extensively in the laboratory [Saville (11), Bowen et al. (12)] and tide gage measurements during severe storms have confirmed its importance in nature. Most of the information relative to wave set-up has been developed for "regular" waves, that is for a wave train in which each wave is the same as the preceding wave. Waves in nature, however, are not regular and tend to occur in groups. An analytic study by Lo (13) has shown that for natural wave trains there is a dynamic wave set-up that is approximately 50% larger than would be predicted by a static treatment. In order to evaluate this result, model studies were conducted in the large University of Florida wave tank. It was found that the experimental and analytical results by Lo were in approximate agreement.

The maximum dynamic wave set-up, η'_{max}, across the surf zone can be shown to be approximately

$$\eta'_{max} = 0.285\left[1 - 2.82\left(\frac{H_b}{gT^2}\right)^{1/2}\right]H_b \qquad (23)$$

which includes the dynamic factor of 50% and in which T is the wave period and H_b is the breaking wave height based on the deep water significant wave height, H_0, taken approximately as

$$H_b = 0.94\,H_0 \qquad (24)$$

The maximum deep water significant wave height, $(H_0)_{max}$, is determined as recommended for hurricane generated waves in the Shore Protection Manual (14),

$$(H_0)_{max} = 16.5e^{R(\Delta p/100)}\left(1 + 0.208\frac{V_F}{\sqrt{W_R}}\right) \qquad (25)$$

where R = radius to maximum winds in nautical miles, Δp = central pressure deficit in inches of mercury, V_F = translation speed of hurricane in knots, and W_R = maximum sustained wind speed in knots. For purposes here, the local effective deep water significant wave height is based on the local winds, W, at the surf zone area of interest and the maximum winds in the hurricane, W_{max}, as

where α_n is the angular deviation of the wind vector from the shore normal. Equations 23, 24, 25 and 26 provide the basis for determining the maximum dynamic wave set-up within the surf zone. The

$$H_0 = (H_0)_{\max}\left(\frac{W}{W_{\max}}\right)^2 \times \begin{cases} \cos\alpha_n, & -\frac{\pi}{2} < |\alpha_n| < \frac{\pi}{2} \\ 0, \text{otherwise} \end{cases} \quad (26)$$

computed value of η'_{max} was added to the nearshore storm surge. It is stressed that η'_{max} represents the maximum dynamic wave set-up across the surf zone and that this value varies with time (because the wind speed varies with time). The value of η'_{max} was computed at each time step for the shoreward grid, and added to the corresponding surge value resulting from wind stress, barometric pressure and the effect of astronomical tide to yield the combined total storm tide history.

With the combined total storm tide history thus determined, it is a simple matter to search in the computer to obtain the maximum of the combined total storm tide at the site of interest.

4.5 Computation of Return Periods

With a sufficient number (591) of maximum combined total storm tides simulated to represent a typical 2,000 year time interval, the tides associated with various return periods of interest are determined. The 591 maximum combined total storm tides are ranked in descending order with the largest occurring first. The return period, TR, of the ranked tides is then

$$\mathrm{TR} = \frac{2000}{\mathrm{M}} \quad (27)$$

in which

TR = Return period in years between expected exceedances of the associated maximum storm tide

M = Rank of maximum storm tide

As an example, for M = 591 (associated with the lowest water level) the return period would be:

$$TR_{591} = 2000/591 = 3.38 \text{ years}$$

which indicates that the smallest storm tide could be expected to be exceeded approximately once every 3.38 years. As a second example, the return period for M = 4 is

$$TR_4 = 2000/4 = 500 \text{ years}$$

The ranked maximum combined total storm tides and associated return periods can be plotted and the combined total storm tide associated with any return period determined. Finally, it is noted that it is possible to run the simulation procedure any number of times to determine the stability (constancy) of any combined total storm tide associated with a given return period. It is expected that for a 2,000 year simulation, the storm tides associated with the longer (> 500 year) return periods would not be well-defined by one simulation and would exhibit variation from simulation to simulation. However, the storm tides associated with the lower return periods (TR < 200 years) should be well-defined by a 2,000 year simulation and hence are not expected to vary significantly for various simulations.

V. CALIBRATION RATIONALE AND RESULTS

5.1 Rationale

Ideally there are sufficient storm tide data (from tide gages) at a site of interest to allow calibration of the numerical model. If this is the case, then it would be possible to calibrate the one-dimensional numerical model with data from the site and it would not be necessary to utilize the two-dimensional model described earlier. Unfortunately, there are not sufficient tide measurements at the site, and it is therefore necessary to utilize the two-dimensional model as an intermediate representation.

The calibration procedure followed is, first, to validate/calibrate the two-dimensional numerical model using tide gage data for hurricanes of September 1926, 1945, 1947 and 1979 (David). With this calibration as a basis for the two-dimensional model, it is then run for a series of hurricanes with parameters encompassing representative ranges. These include 11 cases for landfalling and exiting hurricanes to determine the peak storm tides at the site. These results are then utilized to calibrate the one-dimensional numerical model which is run for the same 11 cases for each of the two types of hurricanes.

5.2 Results--Calibration of Two-Dimensional Numerical Model

The calibration is conducted by running the two-dimensional model for the hurricane characteristics presented in Table I and the results are then compared with the measurements. The data used and the calibration results are as follows:

1. Hurricane of September 1926

   There is no tide gage recordings of this hurricane. The high water mark at Miami Beach as reported by Reference (15) is used to compare the computed storm tide. Figure 20 shows the computed storm tide with the reported high water marks for the Miami Beach area. The computed peak tide level is at about the midpoint of the measured high water mark range of 9 to 11 ft.

Table I

Input Parameters for Calibration Hurricanes

Hurricane of September 1926

date	time (EST)	Δp (in. Hg)	V_F (knots)	R (n. mi.)	θ_N (degrees)
9/17	0100	-2.31	13.88	19.0	115.62
	0700	-2.31	11.83	19.0	114.99
	1300	-2.31	11.03	19.0	116.95
	1900	-2.31	12.29	19.0	119.22
9/18	0100	-2.31	9.79	19.0	114.11
	0700	-2.31	12.29	19.0	119.22
	1300	-1.86	12.29	19.0	119.22

Starting Coordinates:

X_s = 318.68 n. mi.

Y_s = 194.00 n. mi.

Landfalling Coordinates:

X_F = -8.81 n. mi.

Y_F = 60.84 n. mi.

Hurricane of September 1945

date	time (EST)	Δp (in. Hg)	V_F (knots)	R (n. mi.)	θ_N (degrees)
9/14	1300	-1.83	14.69	12.0	114.11
	1900	-1.83	13.08	12.0	117.31
9/15	0100	-1.83	12.29	12.0	119.22
	0700	-1.83	12.07	12.0	125.45
	1300	-1.83	12.00	12.0	131.83
	1900	-1.83	13.12	12.0	146.97
9/16	0100	-1.48	12.52	12.0	163.41

Starting Coordinates:

X_s = 316.15 n. mi.

Y_s = 230.31 n. mi.

Landfalling Coordinates:

X_F = -4.40 n. mi.

Y_F = 73.65 n. mi.

Hurricane of September 1947

date	time (EST)	Δp (in. Hg)	V_F (knots)	R (n. mi.)	θ_N (degrees)
9/16	1300	-1.95	7.15	26.0	90.00
	1900	-1.95	8.11	26.0	82.91
9/17	0100	-1.95	8.99	26.0	83.62
	0700	-1.95	8.29	26.0	76.04
	1300	-1.95	7.43	26.0	74.37
	1900	-1.95	5.36	26.0	90.00
9/18	0100	-1.95	6.57	26.0	107.73

Starting Coordinates:

X_s = 172.94 n. mi.

Y_s = -17.22 n. mi.

Landfalling Coordinates:

X_F = -0.80 n. mi.

Y_F = 15.21 n. mi.

Hurricane David of September 1979

date	time (EST)	Δp (in. Hg)	V_F (knots)	R (n. mi.)	θ_N (degrees)
9/2	1300	-1.01	10.01	27.0	134.93
	1900	-1.10	10.66	27.0	131.03
9/3	0100	-1.15	10.95	27.0	155.92
	0700	-1.18	10.48	27.0	149.21
	1300	-1.21	8.44	27.0	161.47
	1900	-1.24	11.32	27.0	166.30
9/4	0100	-1.27	11.04	20.0	175.35

Starting Coordinates:

X_s = 154.04 n. mi.

Y_s = 152.79 n. mi.

Landfalling Coordinates:

X_F = 7.00 n. mi.

Y_F =-25.62 n. mi.

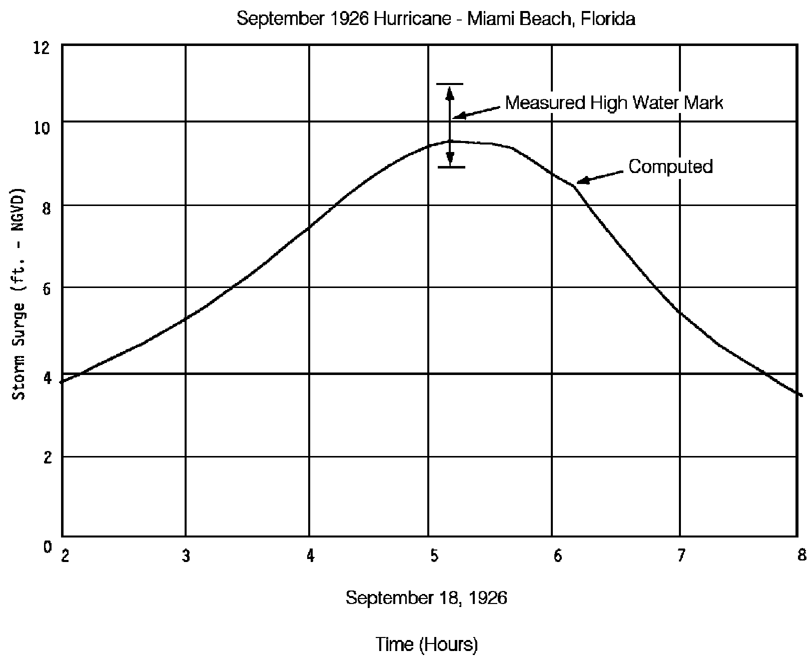

Figure 20 Comparison between Measured and Computed Storm Tide at Miami Beach, Florida for Hurricane of September 1926

2. Hurricane of September 1945

Tide gage recordings during the hurricane are available from Reference (5). Figure 21 shows the tide gage measurement and computed storm tides at Miami Beach. The computed peak tide level is about 0.1 ft. lower than that measured.

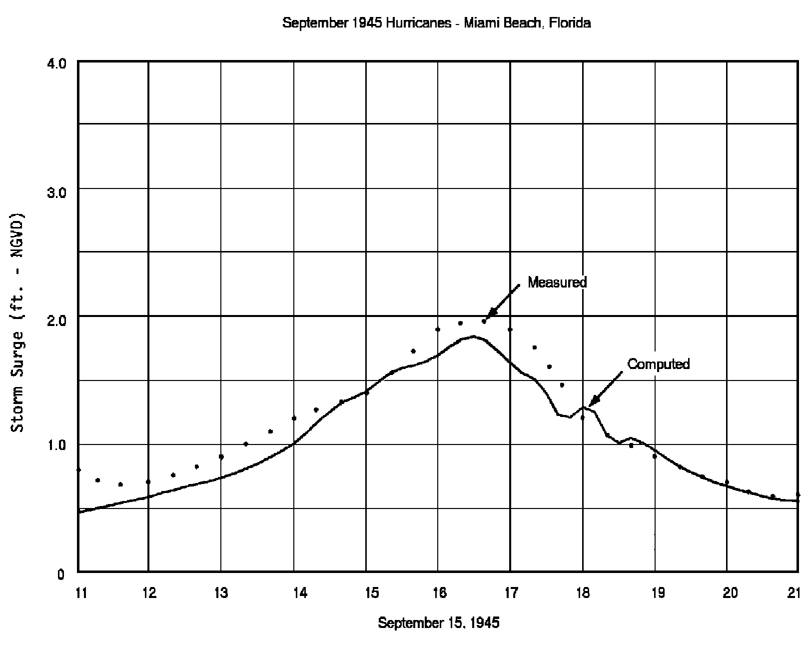

Figure 21 Comparison between Measured and Computed Storm Tide at Miami Beach, Florida for Hurricane of September 1945

3. Hurricane of September 1947

Tide gage recordings at Miami Beach during this hurricane as reported by Reference (15) are shown in Figure 22 along with the computed storm tide. The computed peak tide level is about 1.3 ft. lower than that meaured.

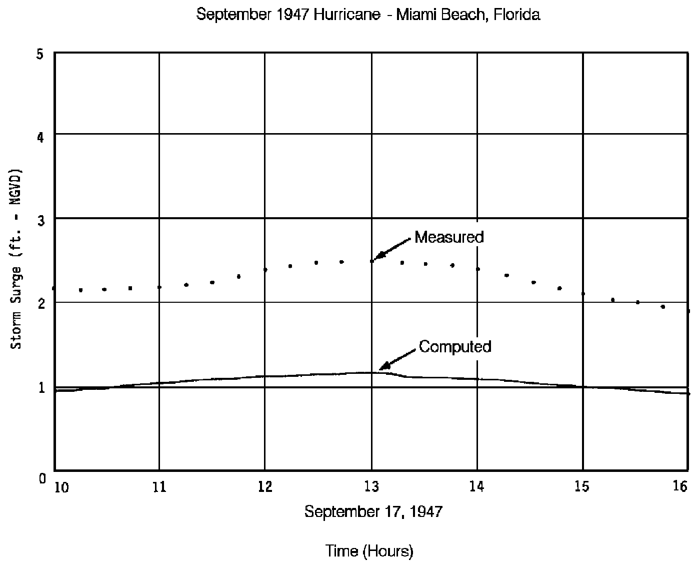

Figure 22 Comparison between Measured and Computed Storm Tide at Miami Beach, Florida for Hurricane of September 1947

4. Hurricane David of September 1979

Figure 23 shows the tide recordings (NOAA) and the computed storm tides at Miami Beach. The computed peak storm tide is about 0.2 ft. higher than the measured at Miami Beach.

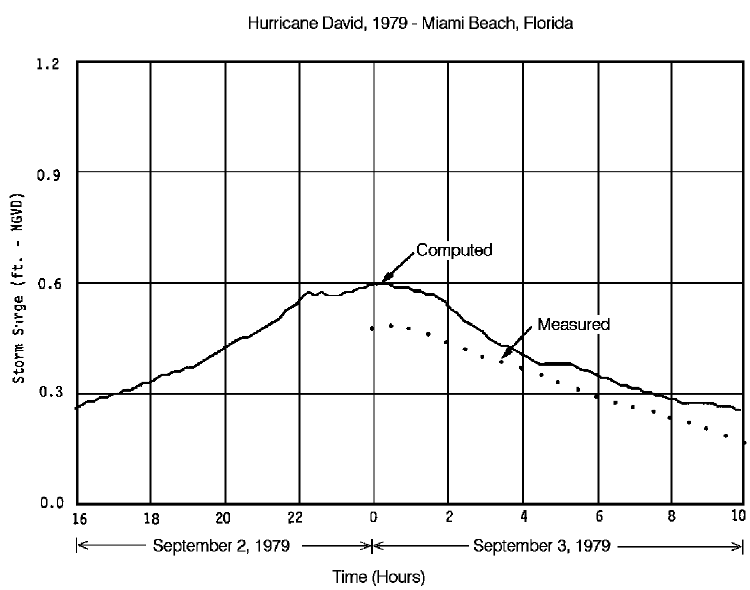

Figure 23 Comparison between Measured and Computed Storm Tide at Miami, Florida for Hurricane David of September 1979

With the comparisons between the measured and computed storm tides for the above four hurricanes, it appears that the two-dimensional model yields reasonably good results. The calibration of the two-dimensional model is thus taken as 1.00, i.e., the calculated storm tides do not have to be adjusted.

5.3 Calibration of One-Dimensional Numerical Model

Eleven cases for each of the two types of hurricanes are run using the two-dimensional model to establish the peak surge at the site of interest. The characteristics of these hurricanes and the peak storm surges at the site are presented in Tables IIa and IIb for landfalling model hurricanes, IIIa and IIIb for exiting hurricanes.

Table IIa

Parameters Defining 11 Landfalling Model Hurricanes Used in Calibrating the One-Dimensional Model with the Two-Dimensional Model

MODEL STORM	Δp (in. Hg)	R (n. mi.)	V_F (knots)	θ_N (degrees)	Landfalling Coordinates (n. mi.) X_F	Landfalling Coordinates (n. mi.) Y_F	Starting Coordinates (n. mi.) X_s	Starting Coordinates (n. mi.) Y_s
1	-1.8	22	11	120	-10	30	119.07	91.56
2	-1.8	32	11	120	-10	30	119.07	91.56
3	-1.8	12	11	120	-10	30	119.07	91.56
4	-1.2	22	11	120	-10	30	119.07	91.56
5	-2.4	22	11	120	-10	30	119.07	91.56
6	-1.8	22	15	120	-10	30	98.31	81.66
7	-1.8	22	7	120	-10	30	84.77	75.20
8	-1.8	22	11	160	-10	30	49.30	160.12
9	-1.8	22	11	80	-10	30	128.45	-5.80
10	-1.8	22	11	120	-10	-20	119.07	41.56
11	-1.8	22	11	120	-10	80	119.07	141.56

Table IIb

Calibration of Landfalling Model Hurricanes

Model Storm	η_{max} (ft. NGVD)							
	Profile One		Profile Two		Profile Three		Profile Four	
	1-D	2-D	1-D	2-D	1-D	2-D	1-D	2-D
1	6.08	6.30	6.86	7.22	7.94	8.44	8.03	8.58
2	8.64	8.97	9.31	9.79	9.71	10.33	7.71	8.41
3	3.40	3.50	4.03	4.22	5.20	5.50	6.96	7.32
4	5.06	5.17	5.84	6.05	6.80	7.11	6.83	7.17
5	7.18	7.52	7.99	8.50	9.21	9.91	9.36	10.12
6	6.56	6.84	7.40	7.80	8.52	9.10	8.59	9.20
7	5.60	5.76	6.32	6.59	7.33	7.74	7.44	7.92
8	6.74	6.88	7.44	7.72	7.83	8.17	8.10	8.42
9	6.47	6.98	6.90	7.54	8.06	8.83	7.23	7.85
10	5.16	5.89	2.04	2.32	1.42	1.60	1.07	1.20
11	3.22	3.25	3.62	3.68	4.18	4.32	4.96	5.15

Table IIIa

Parameters Defining 11 Exiting Model Hurricanes Used in Calibrating the One-Dimensional Model with the Two-Dimensional Model

MODEL STORM	Δp (in. Hg)	R (n. mi.)	V_F (knots)	θ_N (degrees)	Landfalling Coordinates (n. mi.)		Starting Coordinates (n. mi.)	
					X_E	Y_E	X_s	Y_s
1	-1.5	22	13	235	10	40	-120.40	147.50
2	-1.5	32	13	235	10	40	-120.40	147.50
3	-1.5	12	13	235	10	40	-120.40	147.50
4	-1.0	22	13	235	10	40	-120.40	147.50
5	-2.0	22	13	235	10	40	-120.40	147.50
6	-1.5	22	17	235	10	40	-94.94	126.51
7	-1.5	22	9	235	10	40	-94.17	125.87
8	-1.5	22	13	260	10	40	-153.62	82.31
9	-1.5	22	13	210	10	40	-62.76	192.54
10	-1.5	22	13	235	10	-20	-120.40	87.50
11	-1.5	22	13	235	10	100	-120.40	207.50

Table IIIb

Calibration of Exiting Model Hurricanes

Model Storm	η_{max} (ft. NGVD)							
	Profile One		Profile Two		Profile Three		Profile Four	
	1-D	2-D	1-D	2-D	1-D	2-D	1-D	2-D
1	3.54	3.63	3.64	3.69	4.43	4.47	5.39	5.48
2	5.25	5.37	5.29	5.36	6.10	6.16	6.88	6.99
3	1.81	1.85	1.93	1.96	2.52	2.54	3.40	3.44
4	2.76	2.79	2.91	2.92	3.60	3.61	4.41	4.46
5	4.32	4.47	4.37	4.46	5.27	5.35	6.37	6.50
6	3.44	3.50	3.57	3.65	4.37	4.43	5.33	5.43
7	3.62	3.70	3.69	3.75	4.47	4.54	5.41	5.48
8	3.44	3.44	3.79	3.82	4.71	4.75	5.79	5.86
9	4.14	4.30	3.88	4.03	4.45	4.59	5.05	5.19
10	6.28	6.39	5.61	5.66	3.84	3.87	2.75	2.74
11	1.72	1.72	1.66	1.67	1.94	1.95	2.27	2.29

A calibration relationship between the peak surges computed from the one-dimensional numerical model and those from the two-dimensional model is determined as follows. The peak surges computed from these two models are plotted as shown in Figures 24a, 24b, 25a and 25b. The plots in Figure 24a is for landfalling hurricanes at the profile one and two transect lines and Figures 24b is for profile three and four transect lines, respectively. Correspondingly, Figures 25a and 25b is for exiting hurricanes. The relationships between the two computed values are represented by the straight lines in the plots and the associated equations in the insets.

In summary, the overall calibration procedure for the simulation is that presented in Figure 14. Eleven cases each for the landfalling and exiting hurricanes with parameters encompassing representative ranges of their cumulative probability distributions are chosen. Peak storm surges corresponding to four locations along the Palm Beach County shoreline (Figure 14) are calculated for the same 22 hurricanes by both one-dimensional and two-dimensional numerical models. Then, for each of the four transect lines, the calculated peak surges are correlated to establish the relationship between the one-dimensional and two-dimensional model results. This "calibrated" storm surge relationship for each of the four transect lines is then utilized in the simulation as described previously to establish a combined total storm tide. The peak of the combined total storm tide at the site is later ranked with 590 other similarly-determined peaks to establish the various return periods of interest.

LANDFALLING HURRICANES

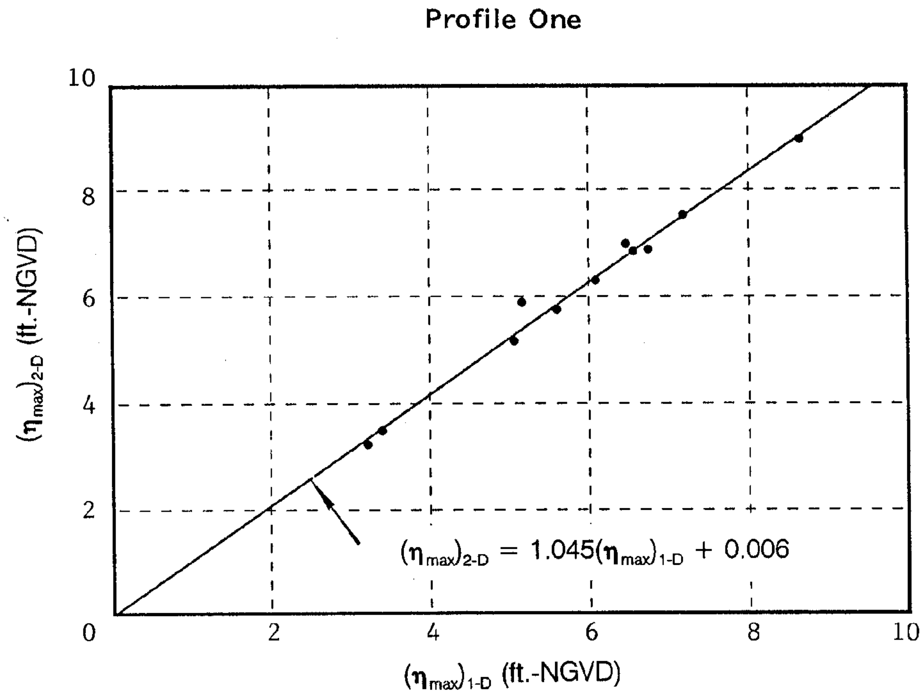

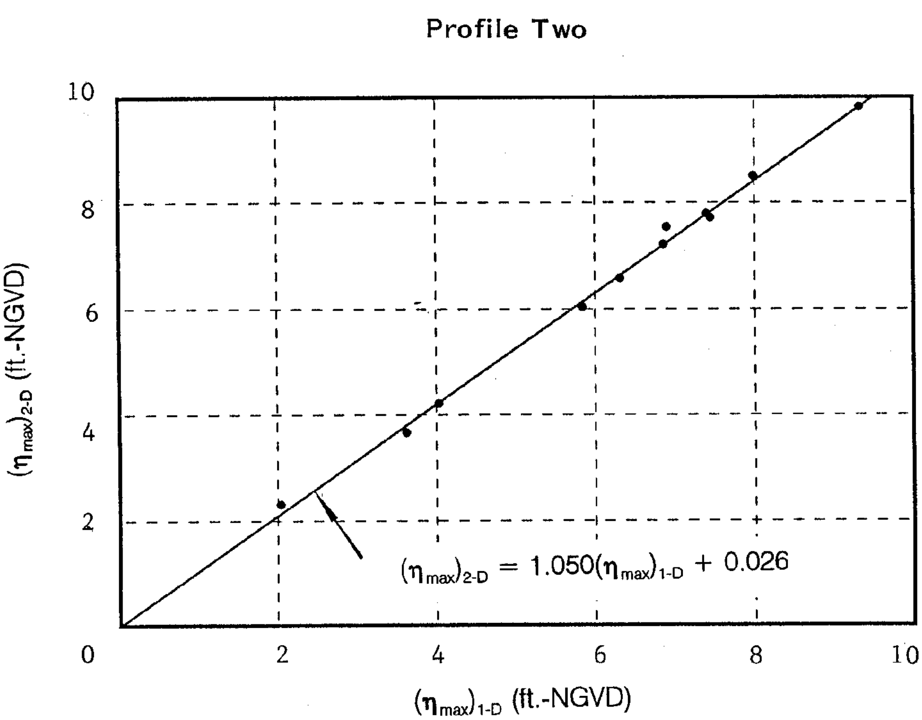

Figure 24a Calibration Relationship between the One-Dimensional and the Two-Dimensional Calculations of Peak Surges at the Profile One and Two Transect Lines of Palm Beach County for Landfalling Hurricanes

LANDFALLING HURRICANES

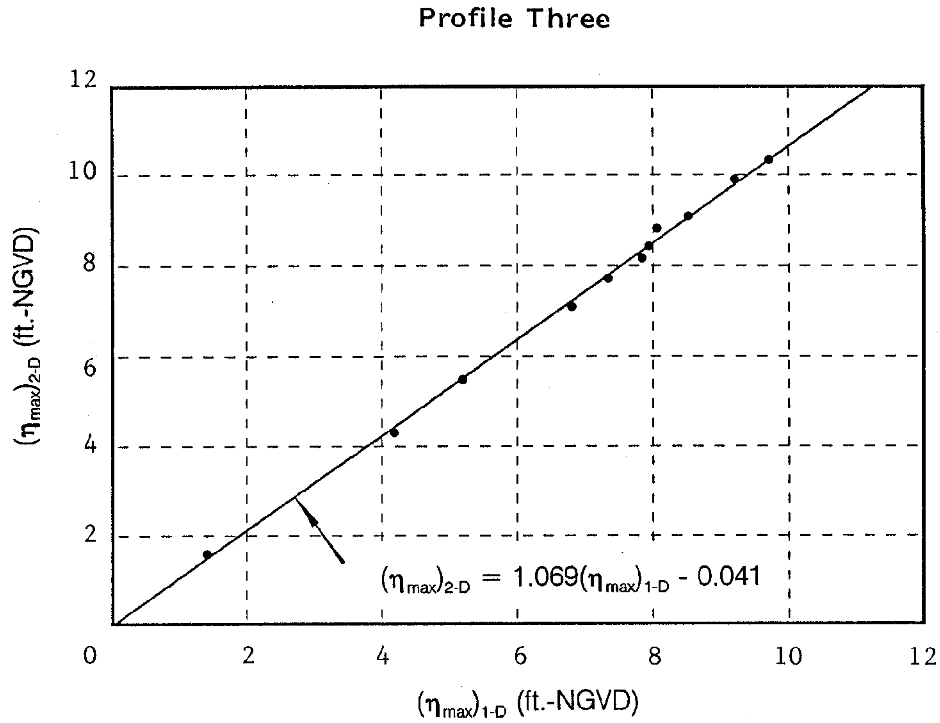

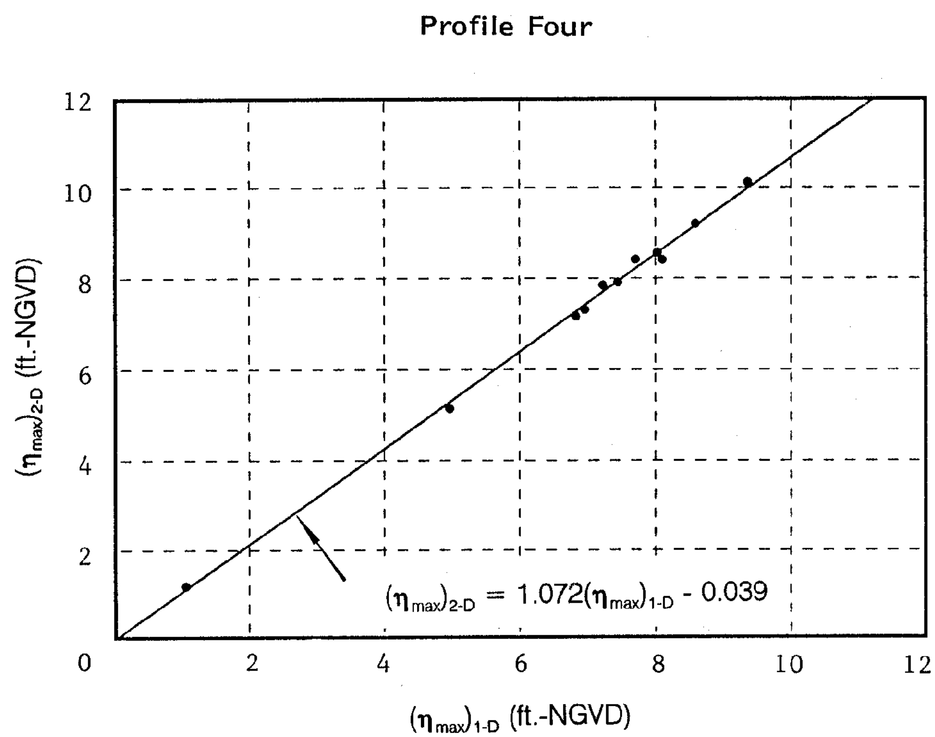

Figure 24b Calibration Relationship between the One-Dimensional and the Two-Dimensional Calculations of Peak Surges at the Profile Three and Four Transect Lines of Palm Beach County for Landfalling Hurricanes

EXITING HURRICANES

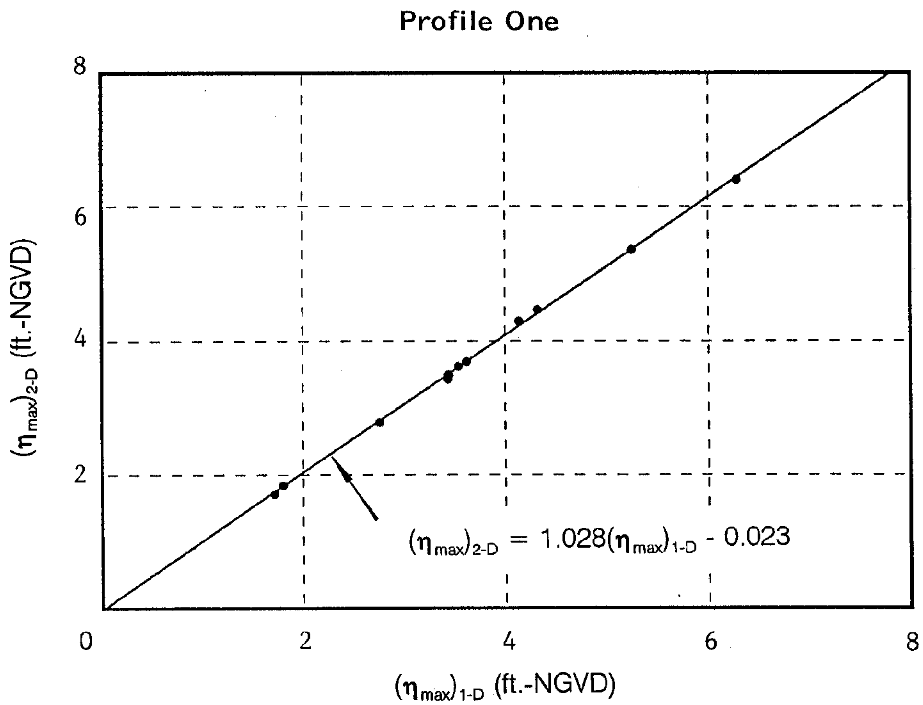

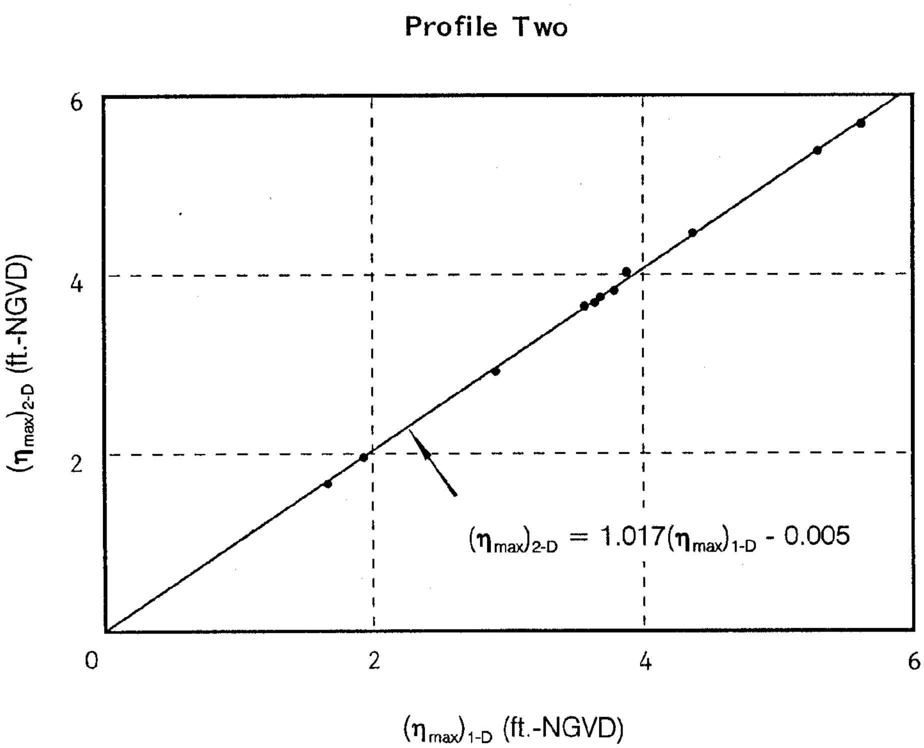

Figure 25a Calibration Relationship between the One-Dimensional and the Two-Dimensional Calculations of Peak Surges at the Profile One and Two Transect Lines of Palm Beach County for Exiting Hurricanes

EXITING HURRICANES

Profile Three

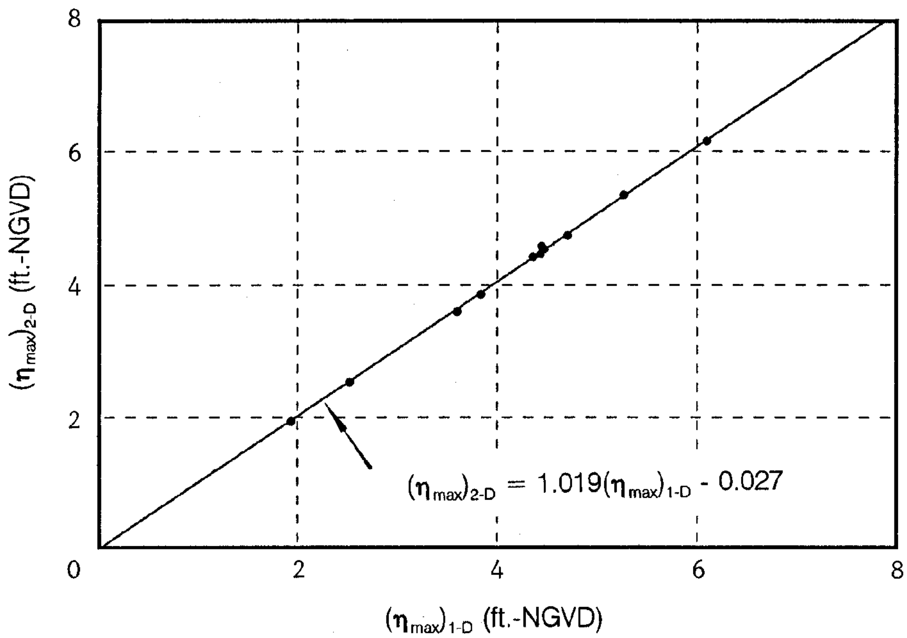

Profile Four

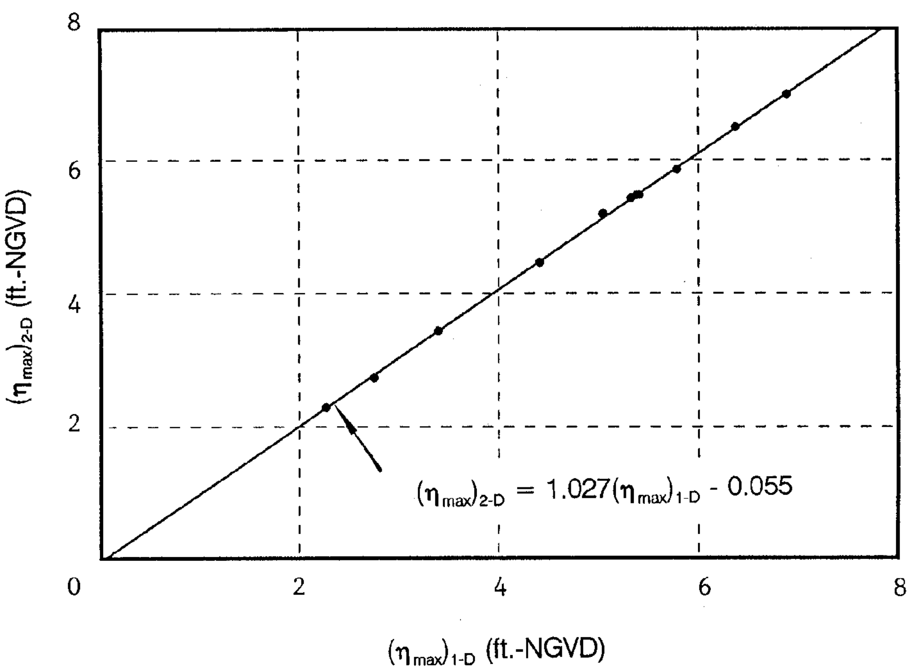

Figure 25b Calibration Relationship between the One-Dimensional and the Two-Dimensional Calculations of Peak Surges at the Profile Three and Four Transect Lines of Palm Beach County for Exiting Hurricanes

VI. RESULTS OF LONG-TERM SIMULATIONS

Five 2,000-year simulations for each of the four transect lines are carried out employing the computer methods and hurricane statistics presented in the preceding sections. The combined total storm tides above NGVD and the associated return periods computed from Equation 27 are plotted on semi-log paper in Figures 26a, 26b, 26c and 26d, respectively for the four transect lines (profiles) along the Palm Beach County shoreline. Each data point on these four figures represents the average value of five simulations and a curve drawn through the data points is adopted to represent the tide-frequency relationship for each of the four transect lines. Figure 27 presents all four combined total storm tide frequency curves depicted in Figures 26a, 26b, 26c and 26d.

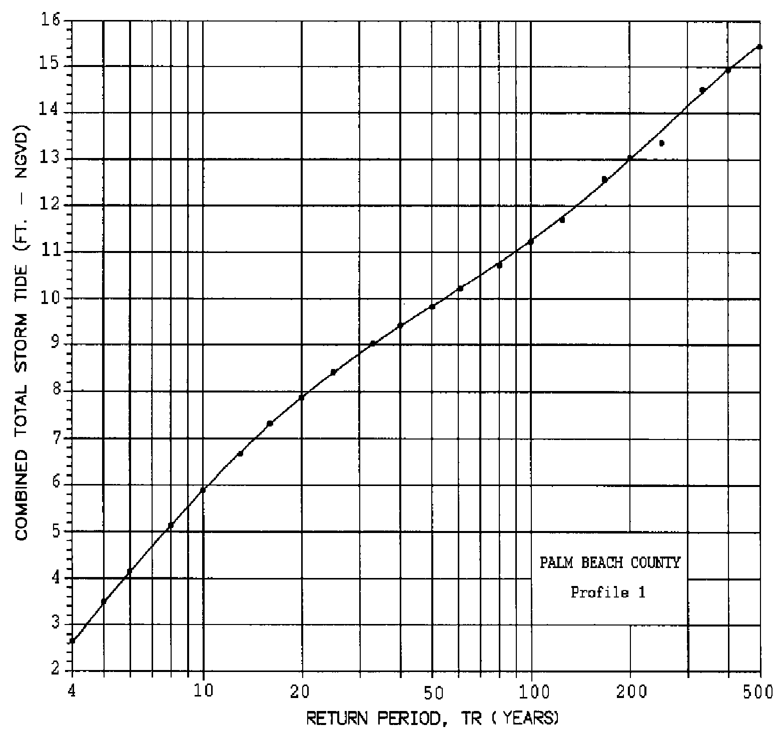

Figure 26a Results of Five 2,000-Year Simulations for the Profile One Transect Line in Palm Beach County

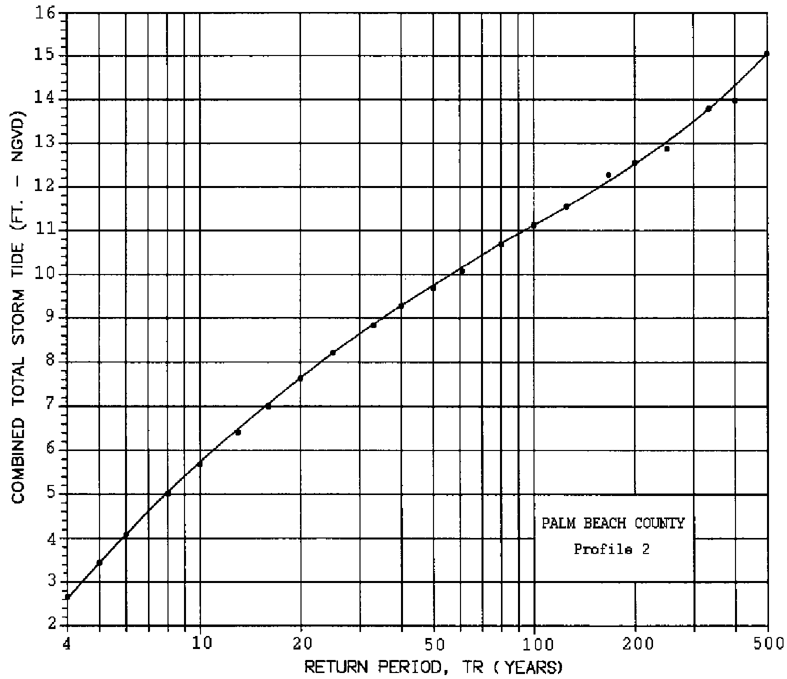

Figure 26b Results of Five 2,000-Year Simulations for the Profile Two Transect Line in Palm Beach County

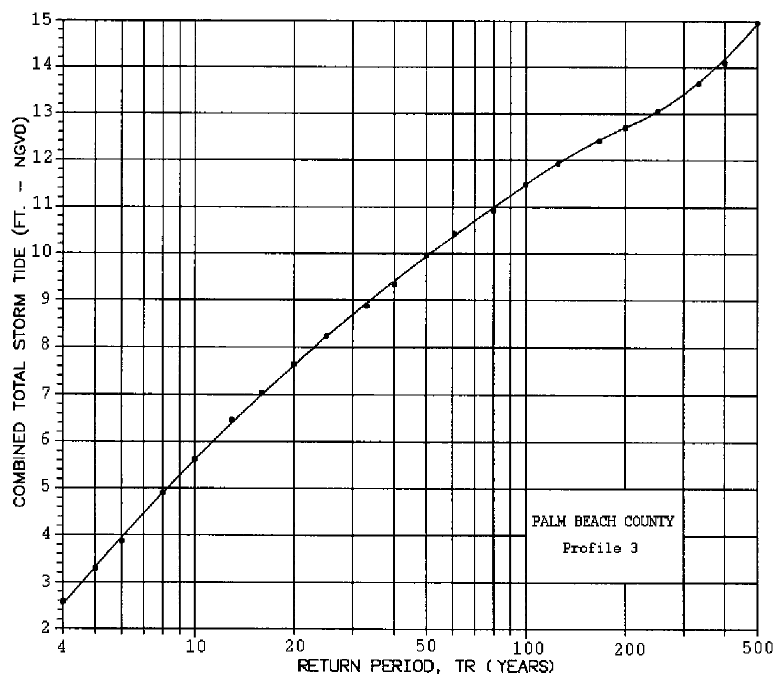

Figure 26c Results of Five 2,000-Year Simulations for the Profile Three Transect Line in Palm Beach County

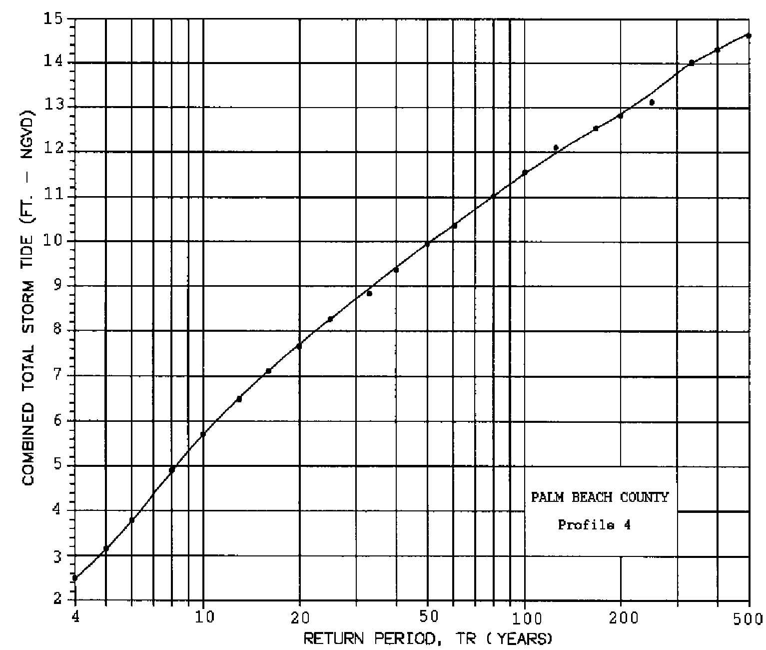

Figure 26d Results of Five 2,000-Year Simulations for the Profile Four Transect Line in Palm Beach County

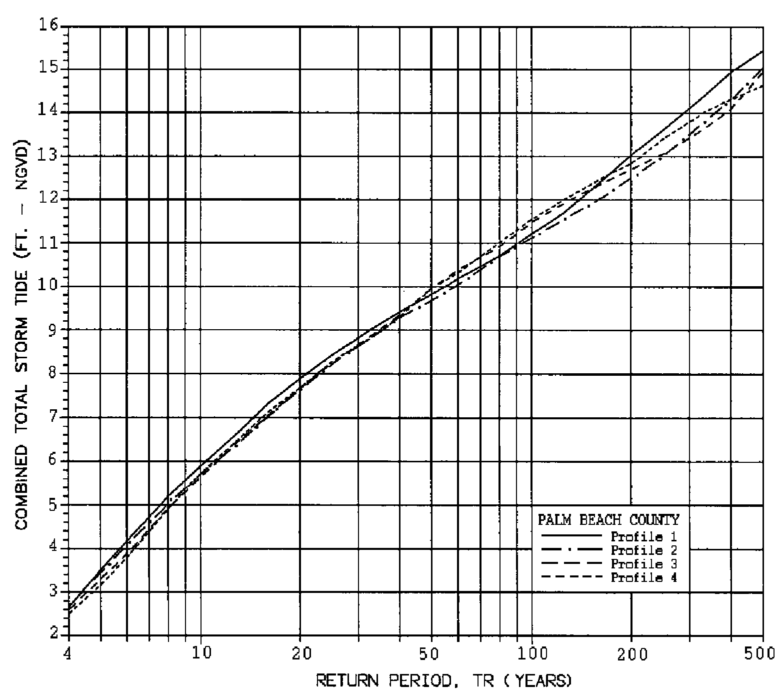

Figure 27 Combined Total Storm Tide Elevation Versus Return Period for the Four Transect Lines in Palm Beach County

Table IV below gives the combined total storm tide values and corresponding return periods for the four transect lines.

Table IV

Combined Total Storm Tide Values for Various Return Periods

Return Period, TR (years)	Combined Total Storm Tide Level* above NGVD (ft.)			
	Profile One	Profile Two	Profile Three	Profile Four
500	15.4	15.0	15.0	14.6
200	13.0	12.5	12.7	12.8
100	11.2	11.1	11.5	11.6
50	9.8	9.7	9.9	9.9
20	7.9	7.6	7.7	7.7
10	5.9	5.7	5.6	5.7
5	3.5	3.4	3.4	3.2

*Includes contributions of: wind stress, barometric pressure, dynamic wave set-up and astronomical tide.

For the purpose of other applications, the selected 100-year frequency storm hydrographs are provided in Appendix C. Table CI and Figure CI is for the profile one transect line, Table CII and Figure CII is for the profile two transect line, Table CIII and Figure CIII is for the profile three transect line and Table CIV and Figure CIV for the profile four transect line in Palm Beach County.

REFERENCES

1. U. S. Army Corps of Engineers, "National Shoreline Study - Regional Inventory Report," South Atlantic Division, Atlanta, Georgia, August 1971.

2. Pilkey, O. H., and et al, "Living with the East Florida Shores," Duke University Press, Durham, North Carolina, 1984.

3. U. S. Army Coups of Engineers, "Beach Erosion Control Study on Palm Beach County, Florida," Jacksonville District, Jacksonville, Florida, November 1964.

4. Florida Department of Natural Resources, "Florida's Beach Restoration Plan for Planning District VII," Chapter II, Report in Preparation.

5. U. S. Department of Commerce, National Oceanic and Atmospheric Administration, "Hurricane Climatology for the Atlantic and Gulf Coasts of the United States," NOAA Technical Report NWS 38, April 1987.

6. U. S. Department of Commerce, National Oceanic and Atmospheric Administration, "A Tropical Cyclone Data Tape for the North Atlantic Basin, 1886-1977: Contents, Limitations and Uses," NOAA Technical Memorandum HWS HC 6, June 1978.

7. Wilson, B. L., "Hurricane Wave Statistics for the Gulf of Mexico," U. S. Army Corps of Engineers, Beach Erosion Board, Technical Memorandum 98, 1956.

8. Van Dorn, W., "Wind Stress on an Artificial Pond," Journal of Marine Research, Volume 12, No. 3, 1953.

9. Christensen, B. A. and Walton, R., "Friction Factors in Flooding Due to Hurricanes," Proceedings, National Symposium on Urban Stormwater Management in Coastal Area, Blacksburg, Virginia, June 19-20, 1980.

10. Freeman, J. C., Jr., Baer, L. and Jung, C. H., "The Bathystrophic Storm Tide," Journal of Marine Research, Volume 16, No. 1, 1957.

11. Saville, T., "Experimental Determination of Wave Set-Up," Proceedings, Second Technical Conference on Hurricanes, pp. 242-252, 1961.

12. Bowen, A. J., Inman, D. L. and Simmons, V. P., "Wave 'Set-Down and Set-Up'," Journal of Geophysical Research, Volume 73, No. 8, pp. 2569-2577, 1968.

13. Lo, J. M., "Dynamic Wave Setup," Paper No. 111, 21st International Conference on Coastal Engineering, Malaga, Spain, June 1988.

14. U. S. Army Corps of Engineers, "Shore Protection Manual, Volumes I, II and III," U. S. Government Printing Office, 1984.

15. Harris, D. L., "Characteristics of the Hurricane Storm Surge," Technical Paper No. 48, U.S. Weather Bureau, Department of Commerce, Washington, D.C., 1963.

APPENDIX A

SUMMARY OF HISTORICAL HURRICANES AFFECTING PALM BEACH COUNTY

SUMMARY OF HISTORICAL HURRICANES AFFECTING PALM BEACH COUNTY

No.	Date	Name	θ_N (degrees)	Y_F (knots)	V_F (in. Hg)	Δp (n. mi.)	R	Type
1	09/09/1903		120.0	-40.0	8.0	-1.08	43.0	L
2	06/14/1906		240.0	-34.0	12.0	-1.01	26.0	E
3	10/11/1906		220.0	27.0	6.0	-1.08	35.0	E
4	10/06/1909		235.0	135.0	10.0	-1.66	22.0	E
5	10/20/1921		260.0	-115.0	10.0	-1.01	MGS	E
6	07/22/1926		150.0	-110.0	8.0	-1.58	14.0	L
7	09/11/1926		110.0	72.0	17.0	-2.43	19.0	L
8	10/14/1926		220.0	99.0	16.0	-2.40	21.0	E
9	08/03/1928		144.0	8.0	6.0	-1.07	MGS	L
10	09/06/1928		120.0	8.0	13.0	-2.30	28.0	L
11	09/21/1929		100.0	101.0	10.0	-1.92	28.0	L
12	08/31/1933		120.0	-7.0	11.0	-1.94	13.0	L
13	08/29/1935		130.0	125.0	9.0	-3.57	6.0	L
14	10/30/1935		60.0	59.0	12.0	-1.19	10.0	L
15	10/03/1941		108.0	90.0	16.0	-1.51	MGS	L
16	09/11/1945		130.0	85.0	10.0	-1.83	12.0	L
17	09/04/1947		80.0	33.0	10.0	-1.96	26.0	L
18	09/18/1948		230.0	-21.0	11.0	-1.47	16.0	E
19	10/03/1948		230.0	59.0	13.0	-1.07	16.0	E
20	08/23/1949		130.0	-7.0	14.0	-1.76	23.0	L
21	10/13/1950	King	150.0	43.0	6.0	-1.72	6.0	L
22	08/29/1960	Donna	138.0	128.0	9.0	-2.46	18.0	L
23	08/20/1964	Cleo	160.0	68.0	9.0	-1.35	7.0	L
24	10/08/1964	Isbell	225.0	-7.0	17.0	-1.05	13.0	E
25	08/26/1965	Betsy	90.0	105.0	11.0	-1.81	22.0	L
26	08/25/1979	David	135.0	-17.0	12.0	-1.33	27.0	L

LANDFALLING - 18 ALONGSHORE - 0 EXITING - 8

APPENDIX B

<u>HURRICANE MODEL</u>

The idealized hurricane model moving at a constant speed V_F at an angle, θ, with respect to the x-axis o the grid system is shown below. The gradient

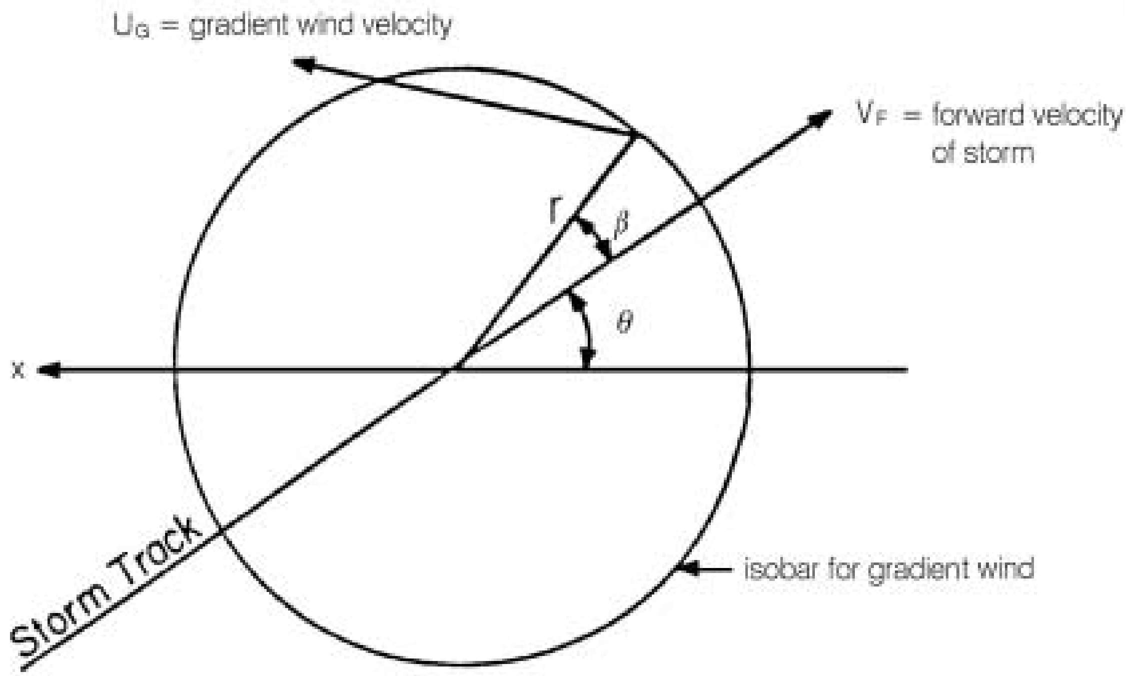

wind speed, U_G (wind speed at 30 ft. above water surface), is calculated by

$$U_G = U_c\left(\sqrt{\gamma^2 + 1} - \gamma\right)\cdot (0.83)$$

where

$$\gamma = \frac{1}{2}\left(\frac{V^1}{U_c} + \frac{U_c}{U_g}\right)$$

and

$$U_c = \sqrt{\frac{\Delta p}{\rho_a}\frac{R}{r}e^{-R/r}}$$

$$U_g = \frac{\frac{\Delta p}{\rho_a}\frac{R}{r^2}e^{-R/r}}{2\omega(\sin\phi)}$$

$2\omega(\sin \phi)$ = Coriolis effect

ω = earth rotation

ϕ = latitude

R = radius to maximum winds

$V' = V_F \sin \beta$

β = angle between observer and hurricane direction

V_F = constant translational speed of hurricane

ρ_a = mass density of air

r = distance from hurricane center to observer

U_g = geostrophic velocity component

U_c = cyclostrophic velocity component.

The factor of 0.83 was applied to the calculation of U_G to take into account friction effects at 30 feet above the water surface.

APPENDIX C

COMPUTED ONE-HUNDRED YEAR HYDROGRAPHS FOR THE FOUR PROFILES IN PALM BEACH COUNTY

TABLE CI

100 Year Frequency Combined Total Storm Tide Hydrograph for Profile One (Range 1 - 60)

Time (hour)	Time Elevation (feet)	Time (hour)	Time Elevation (feet)	Time (hour)	Time Elevation (feet)	Time (hour)	Time Elevation (feet)
0.00	0.07	9.50	4.16	19.00	9.76	28.50	-0.23
0.50	-0.11	10.00	4.00	19.50	7.87	29.00	0.16
1.00	0.19	10.50	3.82	20.00	5.42	29.50	0.57
1.50	0.16	11.00	3.67	20.50	3.54	30.00	0.96
2.00	0.01	11.50	3.57	21.00	3.03	30.50	1.31
2.50	0.24	12.00	3.54	21.50	2.48	31.00	1.60
3.00	0.59	12.50	3.62	22.00	1.93	31.50	1.81
3.50	1.02	13.00	3.82	22.50	1.38	32.00	1.92
4.00	1.50	13.50	4.15	23.00	0.85	32.50	1.93
4.50	2.02	14.00	4.63	23.50	0.34	33.00	1.83
5.00	2.53	14.50	5.25	24.00	-0.12	33.50	1.64
5.50	3.02	15.00	6.00	24.50	-0.51	34.00	1.36
6.00	3.46	15.50	6.88	25.00	-0.83	34.50	1.01
6.50	3.82	16.00	7.83	25.50	-1.05	35.00	0.61
7.00	4.10	16.50	8.82	26.00	-1.17	35.50	0.20
7.50	4.29	17.00	9.77	26.50	-1.17	36.00	-0.21
8.00	4.37	17.50	10.55	27.00	-1.07		
8.50	4.37	18.00	10.98	27.50	-0.86		
9.00	4.30	18.50	10.79	28.00	-0.58		

Figure CI

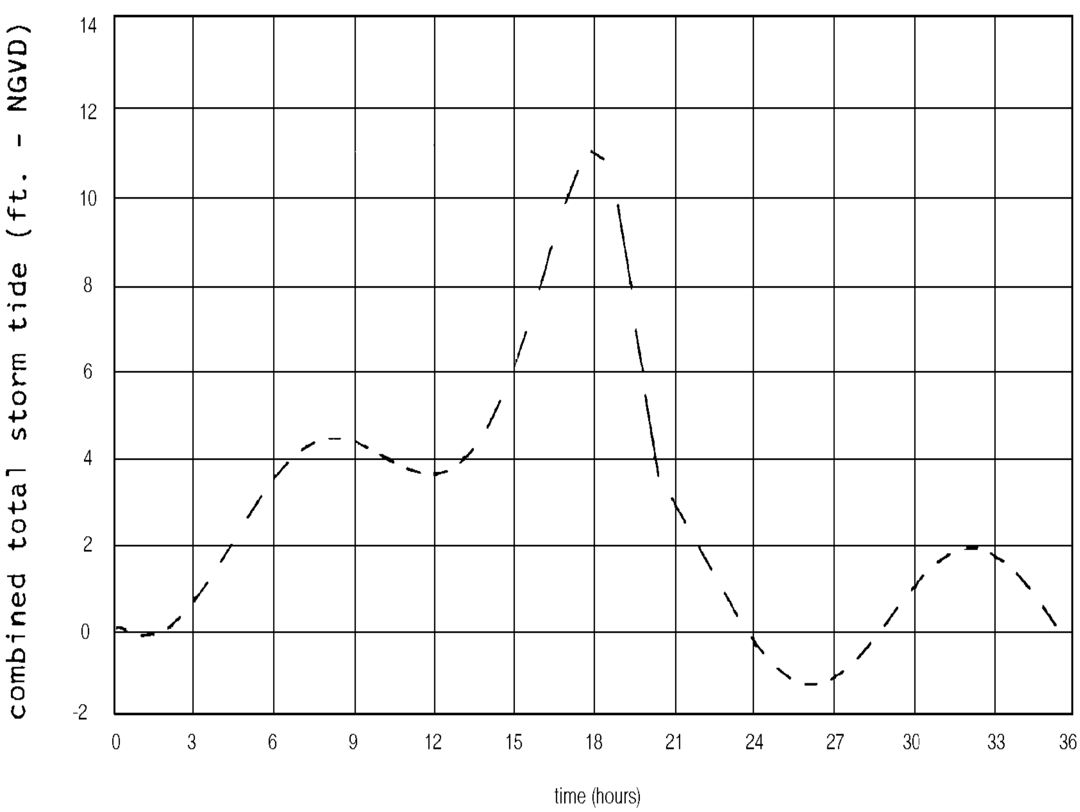

TABLE CII

100 Year Frequency Combined Total Storm Tide Hydrograph for Profile Two (Range 61 - 125)

Time (hour)	Time Elevation (feet)	Time (hour)	Time Elevation (feet)	Time (hour)	Time Elevation (feet)	Time (hour)	Time Elevation (feet)
0.00	2.01	9.50	3.53	19.00	11.05	28.50	2.45
0.50	2.34	10.00	3.75	19.50	10.45	29.00	2.39
1.00	2.67	10.50	4.05	20.00	9.62	29.50	2.26
1.50	2.98	11.00	4.44	20.50	8.59	30.00	2.08
2.00	3.27	11.50	4.91	21.00	7.43	30.50	1.85
2.50	3.51	12.00	5.45	21.50	6.22	31.00	1.58
3.00	3.70	12.50	6.04	22.00	5.03	31.50	1.30
3.50	3.83	13.00	6.68	22.50	3.95	32.00	1.00
4.00	3.91	13.50	7.35	23.00	3.02	32.50	0.71
4.50	3.92	14.00	8.03	23.50	2.26	33.00	0.45
5.00	3.88	14.50	8.71	24.00	1.68	33.50	0.22
5.50	3.81	15.00	9.35	24.50	1.59	34.00	0.05
6.00	3.70	15.50	9.96	25.00	1.71	34.50	-0.07
6.50	3.58	16.00	10.49	25.50	1.86	35.00	-0.12
7.00	3.47	16.50	10.95	26.00	2.02	35.50	-0.10
7.50	3.38	17.00	11.29	26.50	2.17	36.00	-0.01
8.00	3.33	17.50	11.50	27.00	2.30		
8.50	3.32	18.00	11.56	27.50	2.40		
9.00	3.39	18.50	11.41	28.00	2.45		

Figure CII

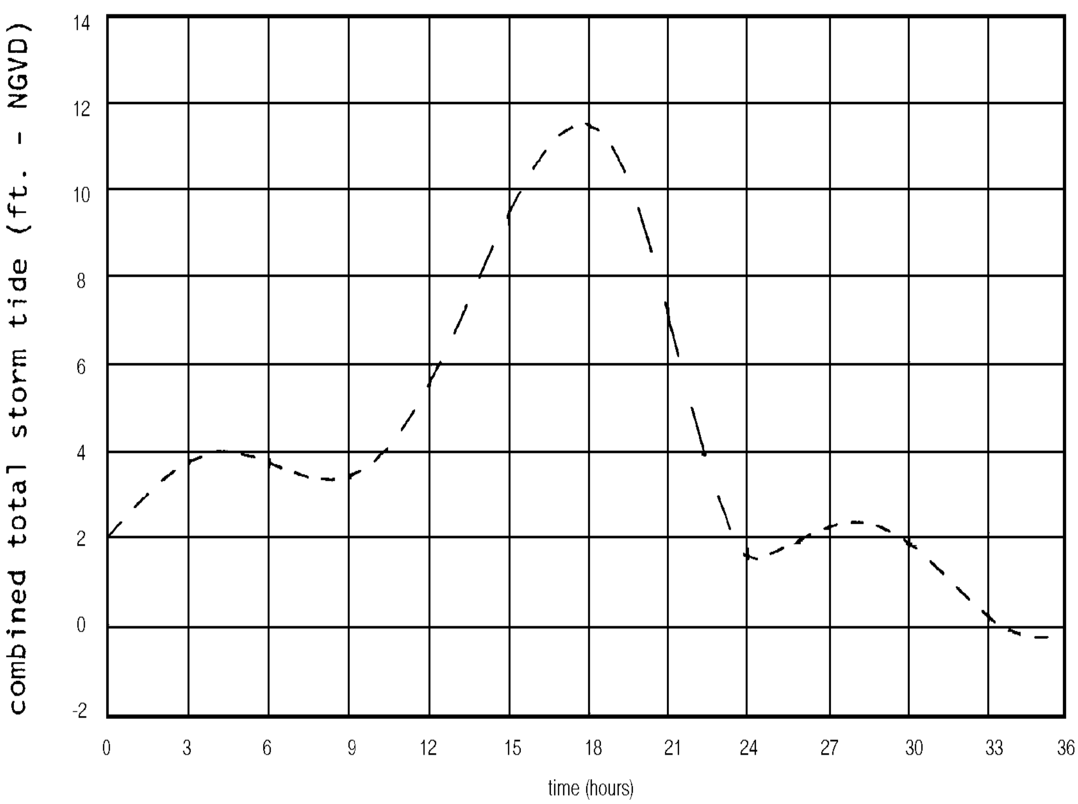

TABLE CIII

100 Year Frequency Combined Total Storm Tide Hydrograph
for Profile Three (Range 126 - 185)

Time (hour)	Time Elevation (feet)	Time (hour)	Time Elevation (feet)	Time (hour)	Time Elevation (feet)	Time (hour)	Time Elevation (feet)
0.00	1.22	9.50	2.15	19.00	10.34	28.50	2.44
0.50	1.64	10.00	2.37	19.50	9.86	29.00	2.28
1.00	2.07	10.50	2.71	20.00	9.16	29.50	2.05
1.50	2.47	11.00	3.16	20.50	8.26	30.00	1.75
2.00	2.84	11.50	3.70	21.00	7.21	30.50	1.39
2.50	3.13	12.00	4.32	21.50	6.08	31.00	1.01
3.00	3.35	12.50	5.01	22.00	4.98	31.50	0.62
3.50	3.49	13.00	5.73	22.50	3.98	32.00	0.25
4.00	3.53	13.50	6.47	23.00	3.14	32.50	-0.08
4.50	3.49	14.00	7.21	23.50	2.48	33.00	-0.36
5.00	3.37	14.50	7.91	24.00	2.01	33.50	-0.56
5.50	3.19	15.00	8.56	24.50	1.72	34.00	-0.67
6.00	2.96	15.50	9.15	25.00	1.55	34.50	-0.69
6.50	2.72	16.00	9.66	25.50	1.49	35.00	-0.61
7.00	2.48	16.50	10.08	26.00	1.97	35.50	-0.45
7.50	2.27	17.00	10.40	26.50	2.21	36.00	-0.21
8.00	2.11	17.50	10.61	27.00	2.38		
8.50	2.03	18.00	10.68	27.50	2.49		
9.00	2.04	18.50	10.60	28.00	2.51		

Figure CIII

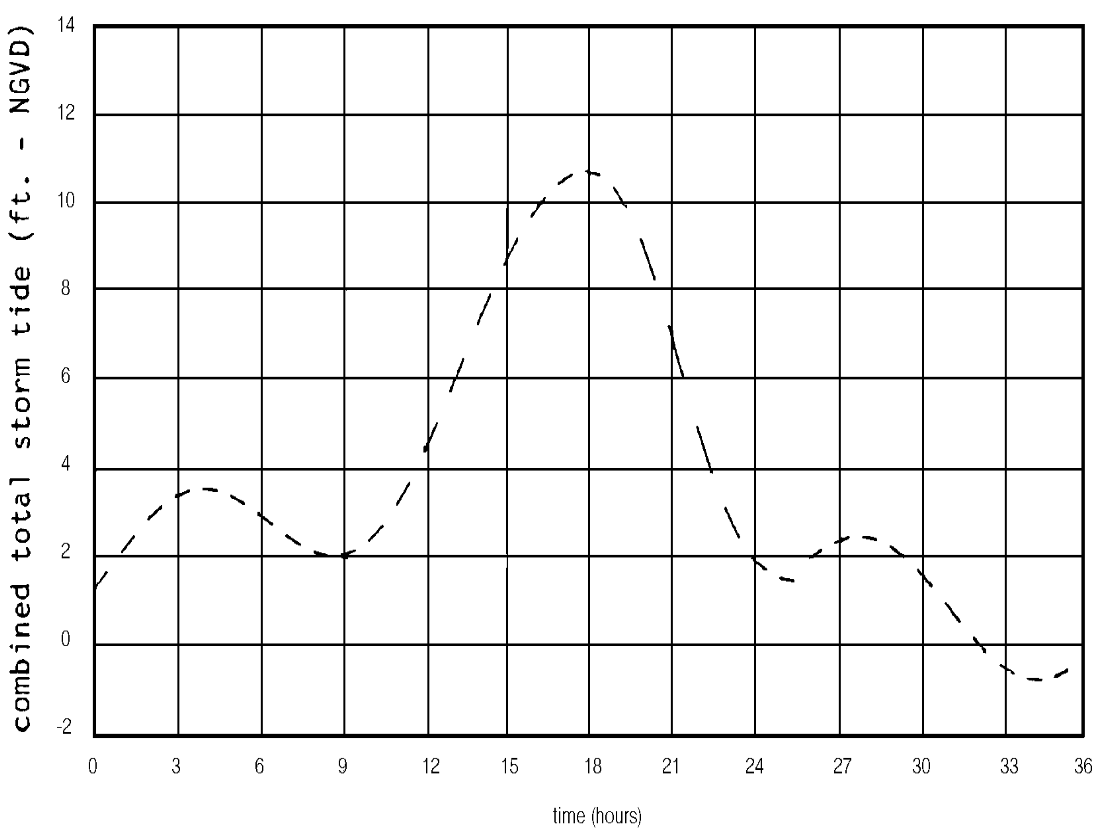

TABLE CIV

100 Year Frequency Combined Total Storm Tide Hydrograph for Profile Four (Range 186 - 227)

Time (hour)	Time Elevation (feet)	Time (hour)	Time Elevation (feet)	Time (hour)	Time Elevation (feet)	Time (hour)	Time Elevation (feet)
0.00	-0.60	9.50	2.45	19.00	11.26	28.50	1.82
0.50	-0.31	10.00	2.33	19.50	10.39	29.00	2.12
1.00	0.08	10.50	2.30	20.00	9.20	29.50	2.33
1.50	0.54	11.00	2.40	20.50	7.80	30.00	2.44
2.00	1.05	11.50	2.62	21.00	6.30	30.50	2.44
2.50	1.58	12.00	2.98	21.50	4.82	31.00	2.34
3.00	2.11	12.50	3.49	22.00	3.44	31.50	2.14
3.50	2.60	13.00	4.13	22.50	2.23	32.00	1.85
4.00	3.02	13.50	4.89	23.00	1.23	32.50	1.50
4.50	3.37	14.00	5.75	23.50	0.44	33.00	1.09
5.00	3.62	14.50	6.69	24.00	-0.14	33.50	0.66
5.50	3.76	15.00	7.67	24.50	-0.52	34.00	0.23
6.00	3.80	15.50	8.65	25.00	-0.70	34.50	-0.16
6.50	3.74	16.00	9.59	25.50	-0.34	35.00	-0.50
7.00	3.60	16.50	10.45	26.00	-0.07	35.50	-0.77
7.50	3.40	17.00	11.16	26.50	0.27	36.00	-0.94
8.00	3.15	17.50	11.66	27.00	0.66		
8.50	2.89	18.00	11.88	27.50	1.07		
9.00	2.65	18.50	11.76	28.00	1.46		

Figure CIV